



Jet substructure measurements in CMS experiment

Suman Chatterjee
for the CMS Collaboration

HEPHY Vienna

26/07/2021

EPS-HEP Conference 2021
Hamburg, Germany Online

Email: suman.chatterjee@cern.ch

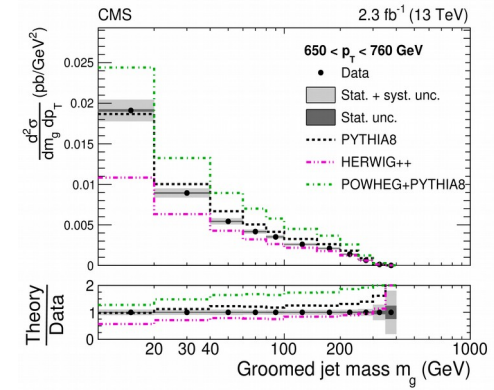


Why jet substructure measurements?

Why jet substructure measurements?

Improved understanding of QCD

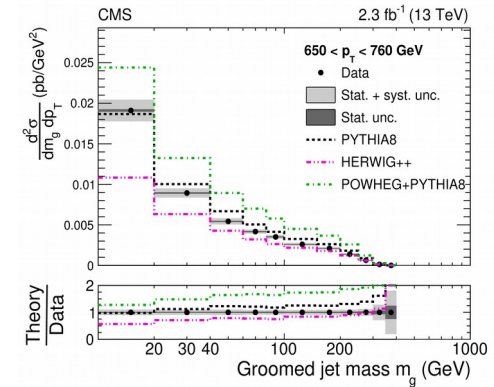
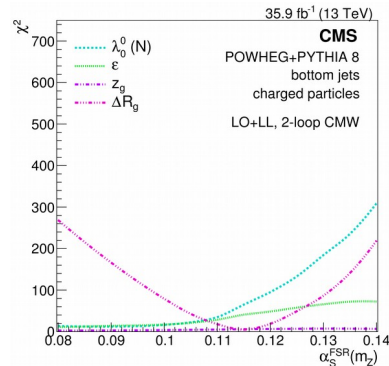
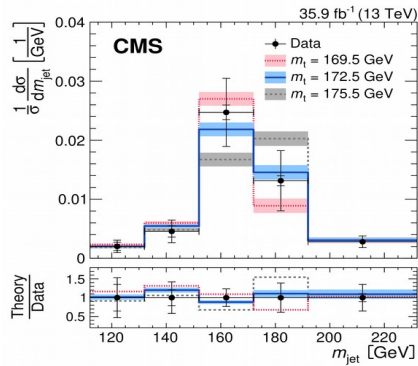
Resummation region enhanced by jet grooming



Why jet substructure measurements?

Improved understanding of QCD

Resummation region enhanced by jet grooming



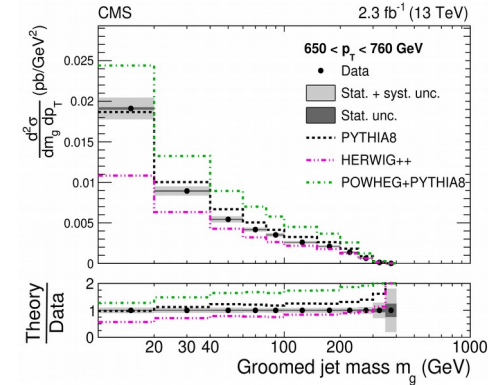
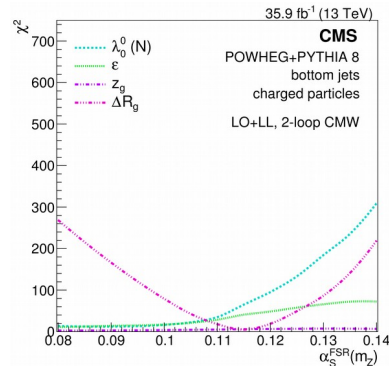
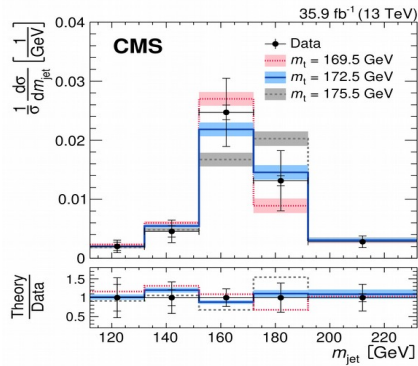
Precision tests of SM parameters
(and probing BSM effects)

α_s running, top quark mass

Why jet substructure measurements?

Improved understanding of QCD

Resummation region enhanced by jet grooming



Precision tests of SM parameters
(and probing BSM effects)

α_s running, top quark mass

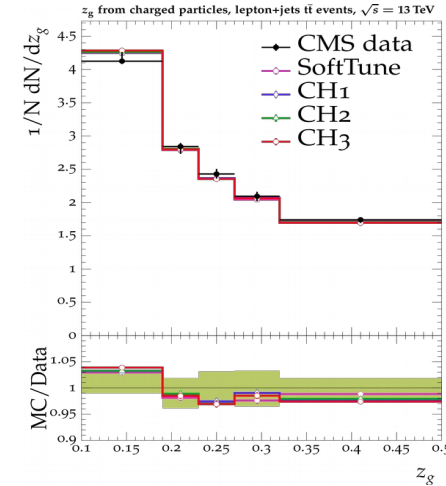
Tuning general purpose MC generators

Understanding parton shower evolution

Improving underlying event description

...

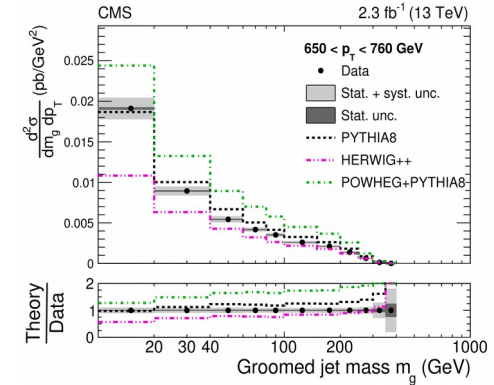
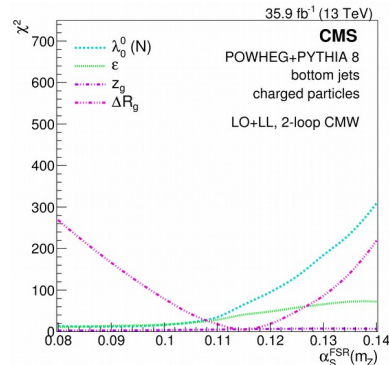
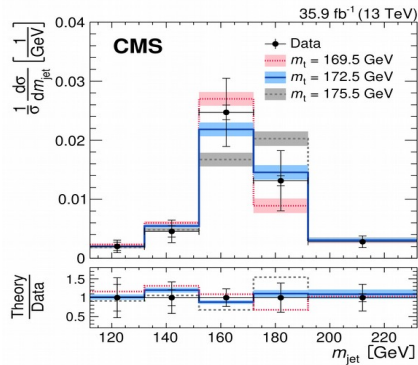
Improves modeling of particle taggers → Helps measurements & searches



Why jet substructure measurements?

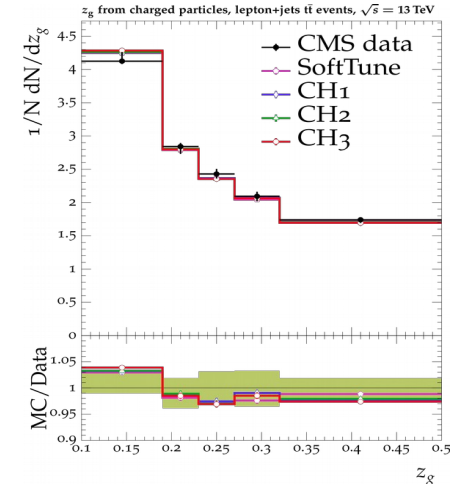
Improved understanding of QCD

Resummation region enhanced by jet grooming



Precision tests of SM parameters
(and probing BSM effects)

α_s running, top quark mass



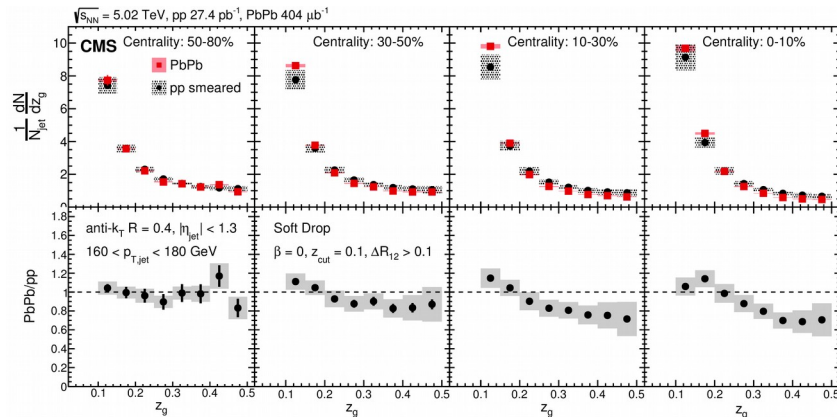
Tuning general purpose MC generators

Understanding parton shower evolution

Improving underlying event description

...

Improves modeling of particle taggers → Helps measurements & searches



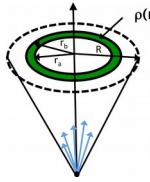
Sensing emergent phenomena

QGP
Dead cone effects

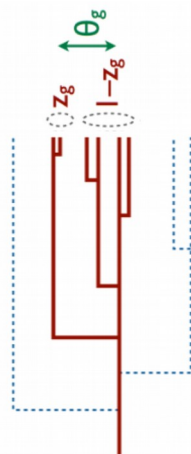
...

Reference	\sqrt{s}	Collision	Events	Jet sample and kinematic region	Observables
1204.3170	7 TeV	pp	Inclusive jets	q/g-jets (AK7), $20 < p_T < 1000$ GeV q/g-jets (AK5), $50 < p_T < 1000$ GeV	Jet shapes, charged hadron multiplicity, width
1205.5872	2.76 TeV	pp/PbPb	Dijet	q/g-jets (AK3), $40 < p_T < 320$ GeV	Jet fragmentation function
1310.0878	2.76 TeV	pp/PbPb	Inclusive jets	q/g-jets (AK3), $100 < p_T < 300$ GeV	Jet fragmentation function
1406.0932	2.76 TeV	pp/PbPb	Inclusive jets	q/g-jets (AK3), $p_T > 100$ GeV	Jet fragmentation function
1310.0878	2.76 TeV	pp/PbPb	Dijet	q/g-jets (AK3), $p_T > 100$ GeV	Jet shapes
1809.08602	2.76 TeV	pp/PbPb	Dijet	q-jets (AK3), $p_T > 30$ GeV	Jet shapes
HIN-19-003	2.76 TeV	pp/PbPb	Dijet	q/g-jets (AK4), $p_T > 50$ GeV	Jet shapes
QCD-10-041	7 TeV	pp	Dijet	q/g-jets (KT6), $97 < p_T < 1032$ GeV	Subjet multiplicities
1706.05868	8 TeV	pp	Inclusive jets	q/g-jets (AK5), $400 < p_T < 1500$ GeV	Jet charge
2004.00602	5.02 TeV	pp/PbPb	Inclusive jets	q/g-jets (AK4), $p_T > 120$ GeV	Jet charge
1703.06330	8 TeV	pp	$t\bar{t}$	top-jets (CA12), $p_T > 400$ GeV	Jet mass
1303.4811	8 TeV	pp	Dijet + W/Z jet	q/g-jets (AK7), $220 < p_T < 1500$ GeV q-jets (AK7, CA8/12), $125 < p_T < 450$ GeV	Nominal + groomed (trimming, pruning, filtering) jet mass
1805.05145	5.02 TeV	pp/PbPb	Inclusive jets	q/g-jets (AK4), $140 < p_T < 300$ GeV	Soft-drop jet mass
1807.05974	13 TeV	pp	Dijet	q/g-jets (AK8), $200 < p_T < 3000$ GeV	Nominal + soft-drop jet mass
1911.03800	13 TeV	pp	$t\bar{t}$	top-jets (XC12), $p_T > 400$ GeV	Xcone groomed jet mass
1708.09429	5.02 TeV	pp/PbPb	Inclusive jets	q/g-jets (AK4), $140 < p_T < 500$ GeV	Soft-drop splitting function
1808.07340	13 TeV	pp	$t\bar{t}$	q-jets (AK4), $p_T > 30$ GeV g-jets (AK4), $p_T > 30$ GeV b-jets (AK4), $p_T > 30$ GeV	Jet substructure and soft-drop observables
SMP-20-010	13 TeV	pp	Dijet, Z+jets	q/g-jets (AK4), $50 < p_T < 4000$ GeV q-jets (AK4), $50 < p_T < 4000$ GeV	Jet angularities

$$z = \frac{p_{\parallel}^{\text{track}}}{p^{\text{jet}}}, \quad \xi = \ln \frac{1}{z}$$

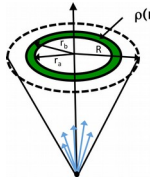


List of jet substructure measurements in CMS

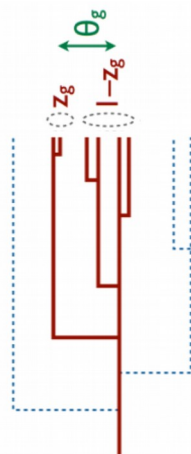


Reference	\sqrt{s}	Collision	Events	Jet sample and kinematic region	Observables
1204.3170	7 TeV	pp	Inclusive jets	q/g-jets (AK7), $20 < p_T < 1000$ GeV q/g-jets (AK5), $50 < p_T < 1000$ GeV	Jet shapes, charged hadron multiplicity, width
1205.5872	2.76 TeV	pp/PbPb	Dijet	q/g-jets (AK3), $40 < p_T < 320$ GeV	Jet fragmentation function
1310.0878	2.76 TeV	pp/PbPb	Inclusive jets	q/g-jets (AK3), $100 < p_T < 300$ GeV	Jet fragmentation function
1406.0932	2.76 TeV	pp/PbPb	Inclusive jets	q/g-jets (AK3), $p_T > 100$ GeV	Jet fragmentation function
1310.0878	2.76 TeV	pp/PbPb	Dijet	q/g-jets (AK3), $p_T > 100$ GeV	Jet shapes
1809.08602	2.76 TeV	pp/PbPb	Dijet	q-jets (AK3), $p_T > 30$ GeV	Jet shapes
HIN-19-003	2.76 TeV	pp/PbPb	Dijet	q/g-jets (AK4), $p_T > 50$ GeV	Jet shapes
QCD-10-041	7 TeV	pp	Dijet	q/g-jets (KT6), $97 < p_T < 1032$ GeV	Subjet multiplicities
1706.05868	8 TeV	pp	Inclusive jets	q/g-jets (AK5), $400 < p_T < 1500$ GeV	Jet charge
2004.00602	5.02 TeV	pp/PbPb	Inclusive jets	q/g-jets (AK4), $p_T > 120$ GeV	Jet charge
1703.06330	8 TeV	pp	$t\bar{t}$	top-jets (CA12), $p_T > 400$ GeV	Jet mass
1303.4811	8 TeV	pp	Dijet + W/Z jet	q/g-jets (AK7), $220 < p_T < 1500$ GeV q-jets (AK7, CA8/12), $125 < p_T < 450$ GeV	Nominal + groomed (trimming, pruning, filtering) jet mass
1805.05145	5.02 TeV	pp/PbPb	Inclusive jets	q/g-jets (AK4), $140 < p_T < 300$ GeV	Soft-drop jet mass
1807.05974	13 TeV	pp	Dijet	q/g-jets (AK8), $200 < p_T < 3000$ GeV	Nominal + soft-drop jet mass
1911.03800	13 TeV	pp	$t\bar{t}$	top-jets (XC12), $p_T > 400$ GeV	Xcone groomed jet mass
1708.09429	5.02 TeV	pp/PbPb	Inclusive jets	q/g-jets (AK4), $140 < p_T < 500$ GeV	Soft-drop splitting function
1808.07340	13 TeV	pp	$t\bar{t}$	q-jets (AK4), $p_T > 30$ GeV g-jets (AK4), $p_T > 30$ GeV b-jets (AK4), $p_T > 30$ GeV	Jet substructure and soft-drop observables

$$z = \frac{p_{\parallel}^{\text{track}}}{p^{\text{jet}}}, \quad \xi = \ln \frac{1}{z}$$



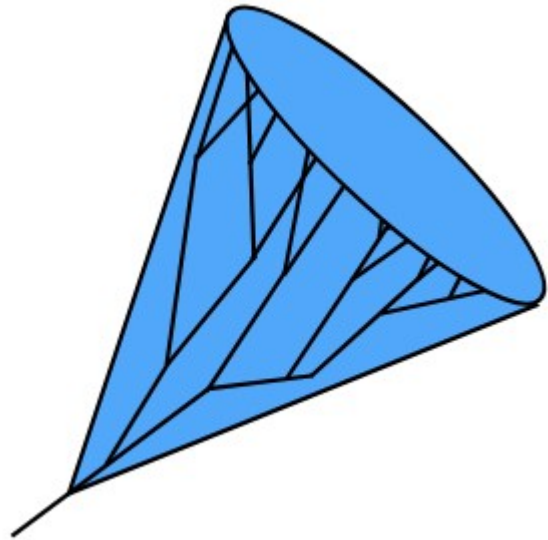
List of jet substructure measurements in CMS



Highlight of today's talk

SMP-20-010	13 TeV	pp	Dijet, Z+jets	q/g-jets (AK4), $50 < p_T < 4000$ GeV q-jets (AK4), $50 < p_T < 4000$ GeV	Jet angularities
------------	--------	----	---------------	--	------------------

Jet substructure measurements in CMS



Observables

Generalized angularities

$$\lambda_{\beta}^{\kappa} = \sum_{i \in \text{jet}} (z_i)^{\kappa} (\theta_i)^{\beta}$$

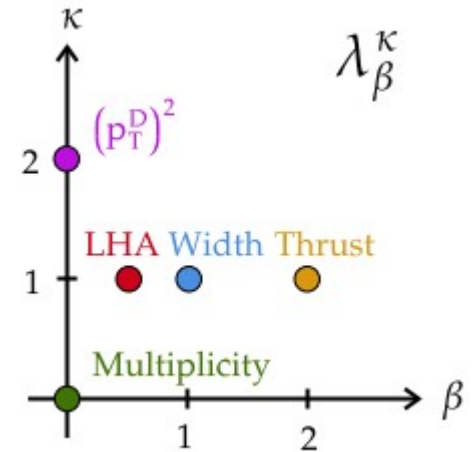
$$z_i = p_{T_i} / \sum p_{T_j}$$

$$\theta_i = \Delta R_{i, \hat{n}} / R_{\text{jet}}$$

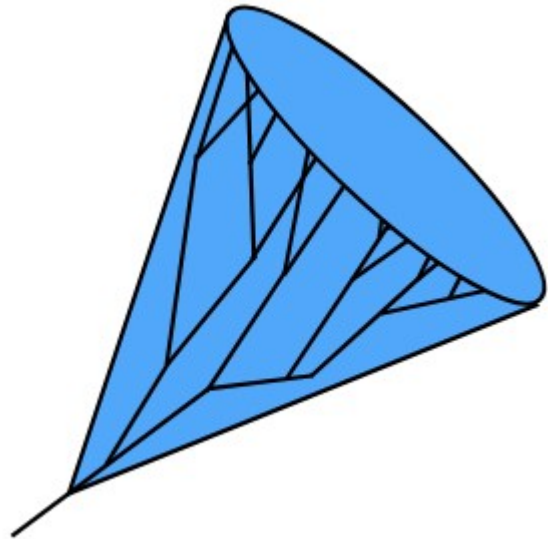
n: jet axis

$\beta \leq 1$: Winner-takes-all (WTA) axis

$\beta > 1$: Anti- k_T axis



Jet substructure measurements in CMS



Observables

Generalized angularities

$$\lambda_{\beta}^{\kappa} = \sum_{i \in \text{jet}} (z_i)^{\kappa} (\theta_i)^{\beta}$$

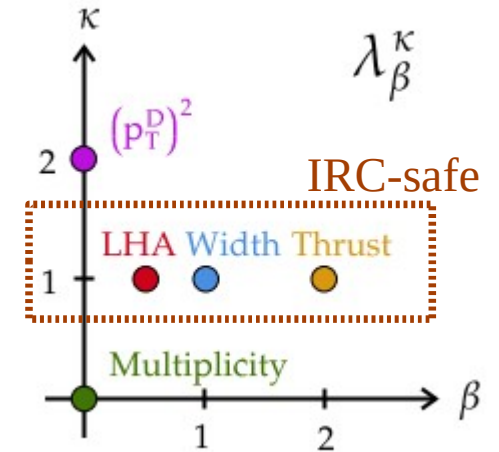
$$z_i = p_{T_i} / \sum p_{T_j}$$

$$\theta_i = \Delta R_{i, \hat{n}} / R_{\text{jet}}$$

n: jet axis

$\beta \leq 1$: Winner-takes-all (WTA) axis

$\beta > 1$: Anti- k_T axis



Jet substructure measurements in CMS

Observables

Generalized angularities

$$\lambda_{\beta}^{\kappa} = \sum_{i \in \text{jet}} (z_i)^{\kappa} (\theta_i)^{\beta}$$

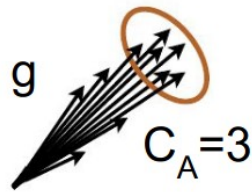
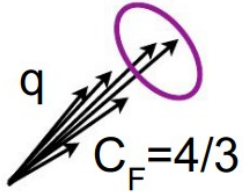
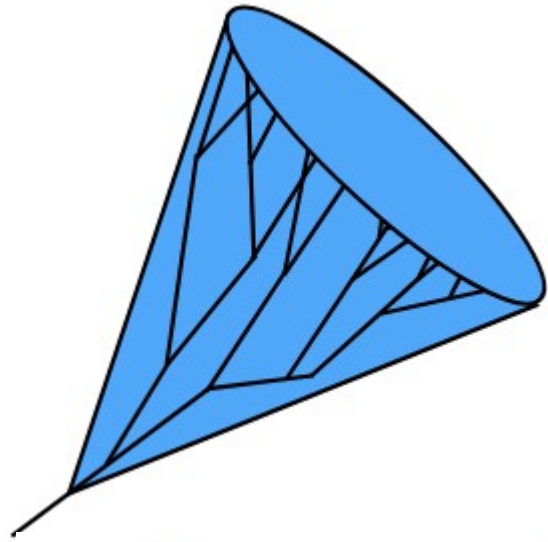
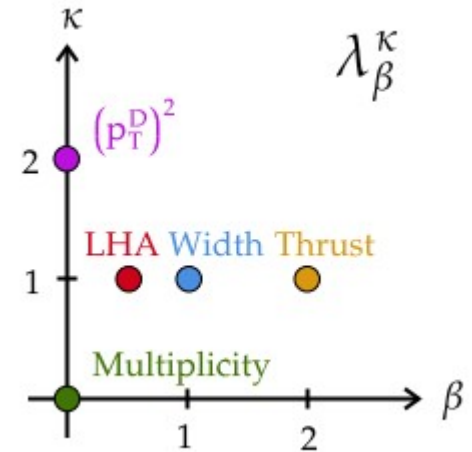
$$z_i = p_{T_i} / \sum p_{T_j}$$

$$\theta_i = \Delta R_{i, \hat{n}} / R_{\text{jet}}$$

n: jet axis

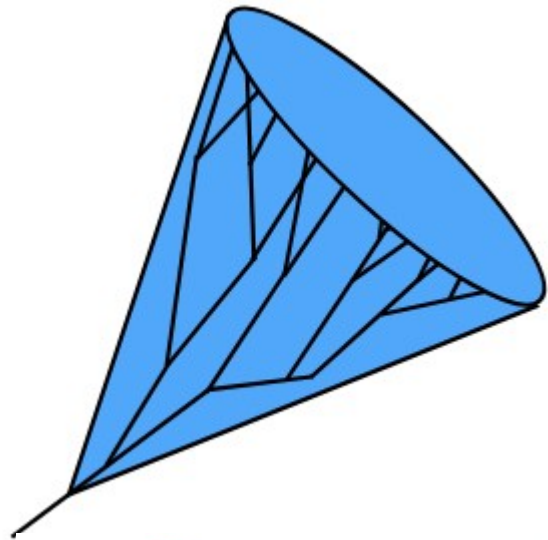
$\beta \leq 1$: Winner-takes-all (WTA) axis

$\beta > 1$: Anti- k_T axis



← Sensitive to differences between quark & gluon jets

Jet substructure measurements in CMS



Observables

Generalized angularities

$$\lambda_{\beta}^{\kappa} = \sum_{i \in \text{jet}} (z_i)^{\kappa} (\theta_i)^{\beta}$$

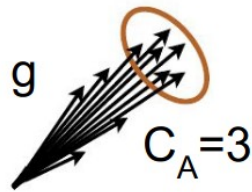
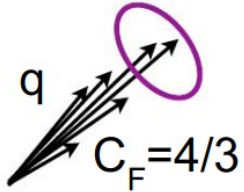
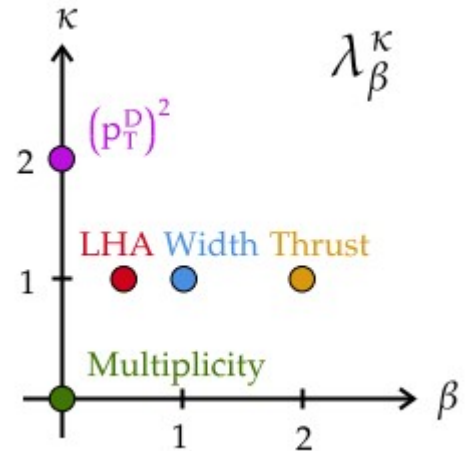
$$z_i = p_{T_i} / \sum p_{T_j}$$

$$\theta_i = \Delta R_{i, \hat{n}} / R_{\text{jet}}$$

n: jet axis

$\beta \leq 1$: Winner-takes-all (WTA) axis

$\beta > 1$: Anti- k_T axis



Measurements: Five λ_{κ}^{β} variables in quark- and gluon-enriched jet samples
(results reported in particle-level)

Study motivated by [JHEP 1707 \(2017\) 091](#) (Gras et al.)

Jet substructure measurements in CMS

Observables

Generalized angularities

$$\lambda_{\beta}^{\kappa} = \sum_{i \in \text{jet}} (z_i)^{\kappa} (\theta_i)^{\beta}$$

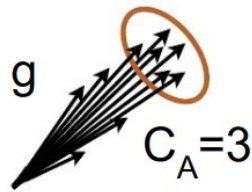
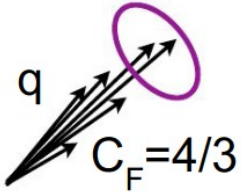
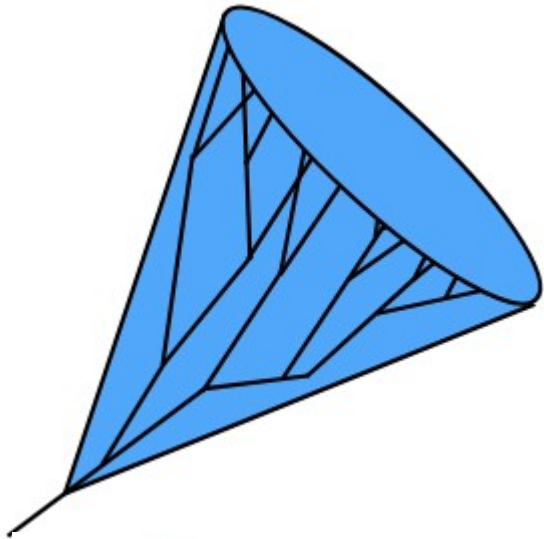
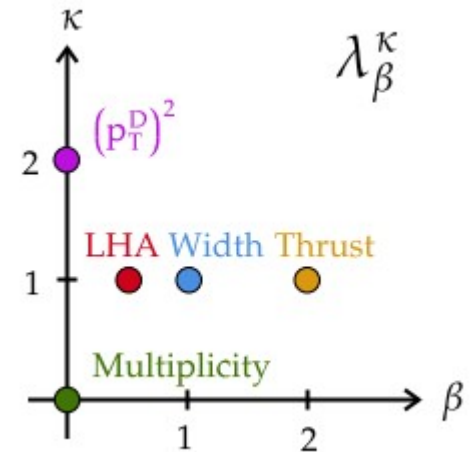
$$z_i = p_{T i} / \sum p_{T j}$$

$$\theta_i = \Delta R_{i, \hat{n}} / R_{\text{jet}}$$

n: jet axis

$\beta \leq 1$: Winner-takes-all (WTA) axis

$\beta > 1$: Anti- k_T axis



Measurements: Five λ_{κ}^{β} variables in quark- and gluon-enriched jet samples
(results reported in particle-level)

Purpose: Detailed understanding of jet composition & its modeling
(not designing a quark-gluon tagger)

Jet substructure measurements in CMS

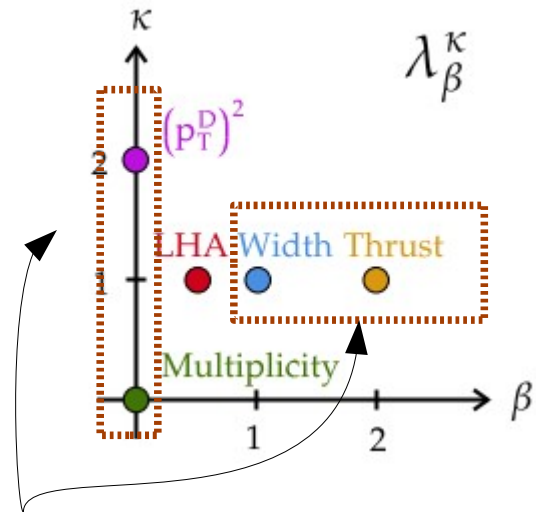
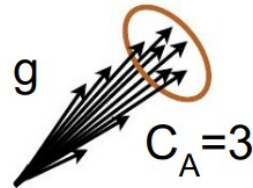
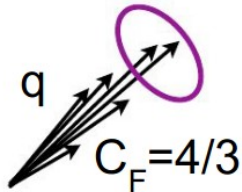
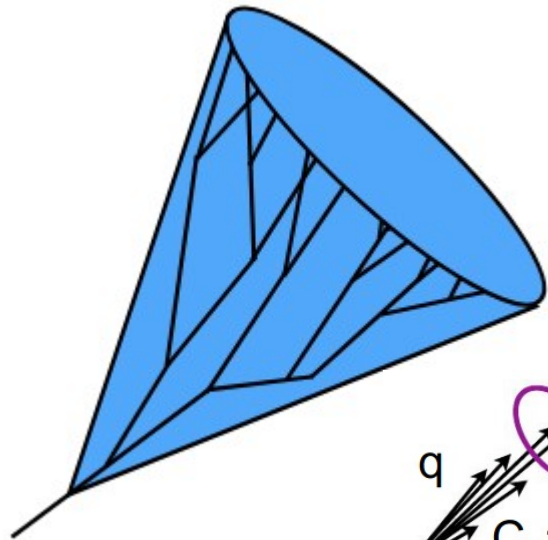
Observables

Generalized angularities

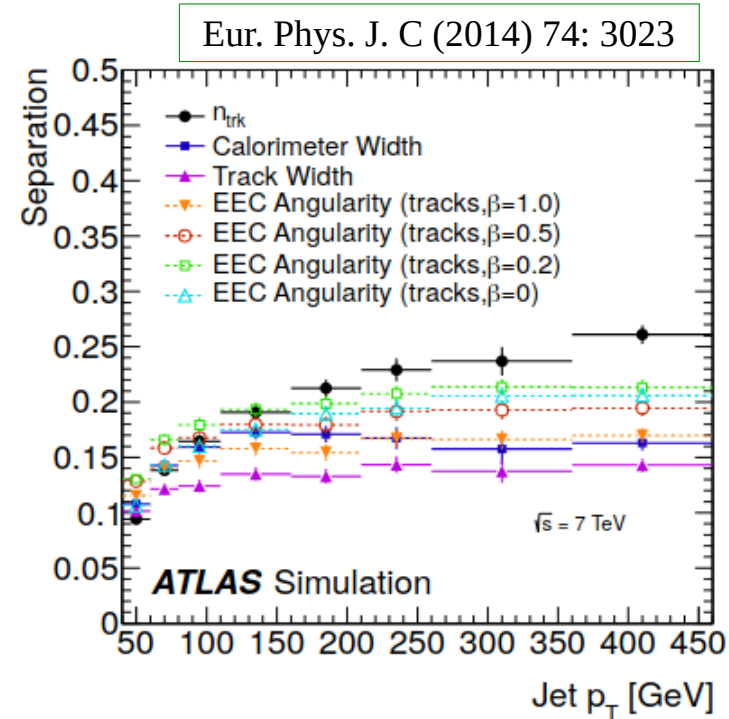
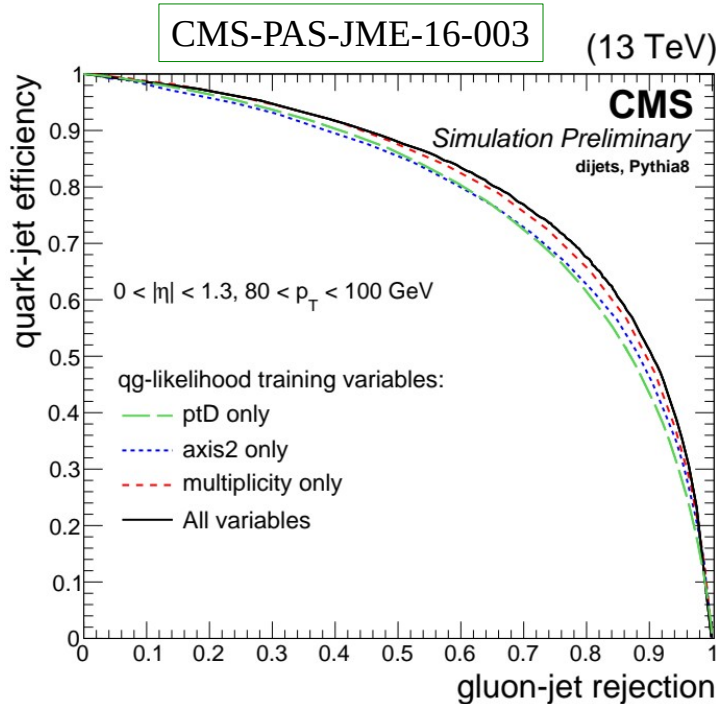
$$\lambda_{\beta}^{\kappa} = \sum_{i \in \text{jet}} (z_i)^{\kappa} (\theta_i)^{\beta}$$

$$z_i = p_{T_i} / \sum p_{T_j}$$

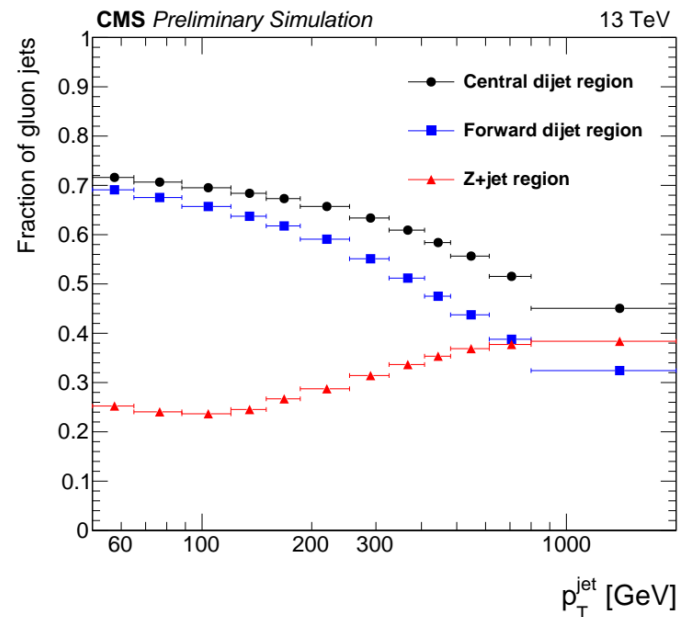
$$\theta_i = \Delta R_{i, \hat{n}} / R_{\text{jet}}$$



Used by experiments for quark-gluon tagging

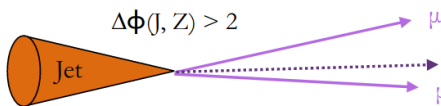


Quark- and gluon-enriched event samples



Quark-enriched jets from Z($\mu\mu$) + jets region:

1+ jets, 2+ muons
 Leading jet must pass p_T , $|y|$ cuts,
 not overlap with Z muons

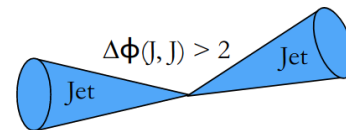


$$|p_T(J) - p_T(Z)| / \sum p_T < 0.3 \quad |m_{\mu\mu} - 90| < 20 \text{ GeV}$$

$$p_{T^{\#\mu}} > 30 \text{ GeV}$$

Gluon-enriched jets from dijet region:

2+ jets
 Leading & subleading jets must pass p_T , $|y|$ cuts



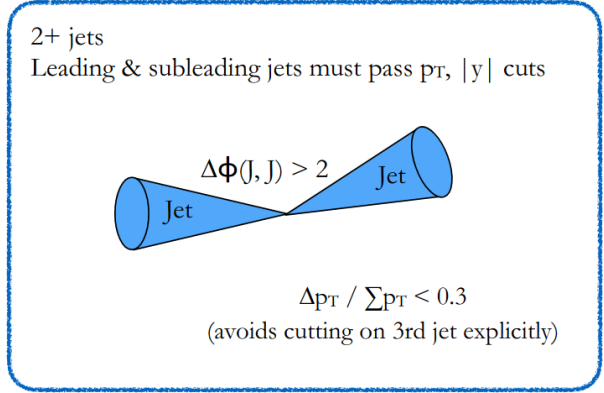
$$\Delta p_T / \sum p_T < 0.3$$

(avoids cutting on 3rd jet explicitly)

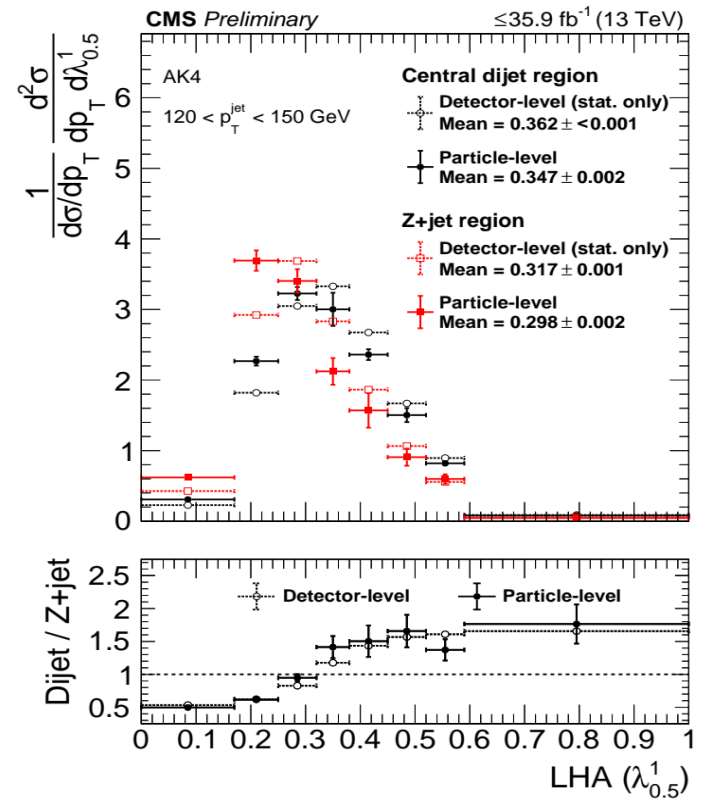
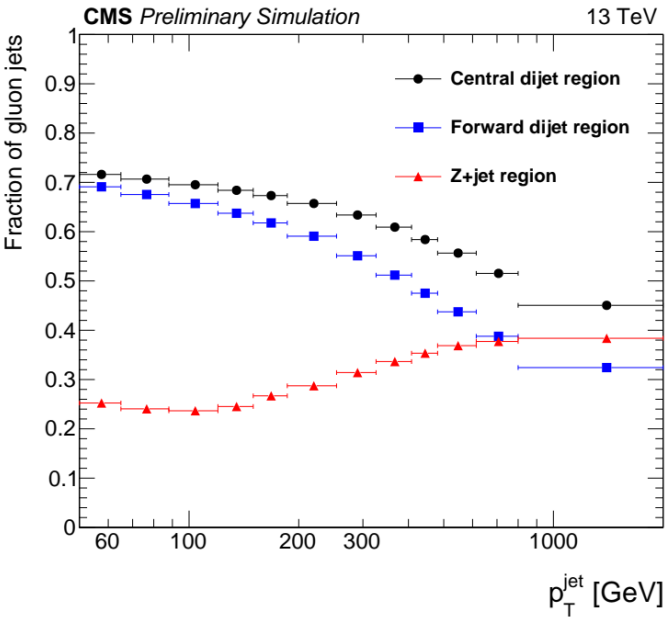
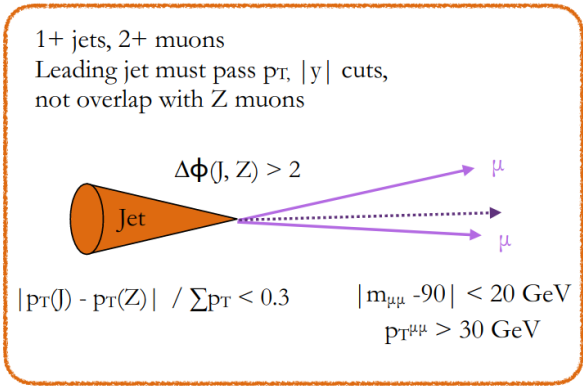
CMS-PAS-SMP-20-010

Quark- and gluon-enriched event samples

Gluon-enriched jets from dijet region:



Quark-enriched jets from Z($\mu\mu$) + jets region:



CMS-PAS-SMP-20-010

Small impact of detector response on ratio



Statistical + systematic uncertainty ~ 5%

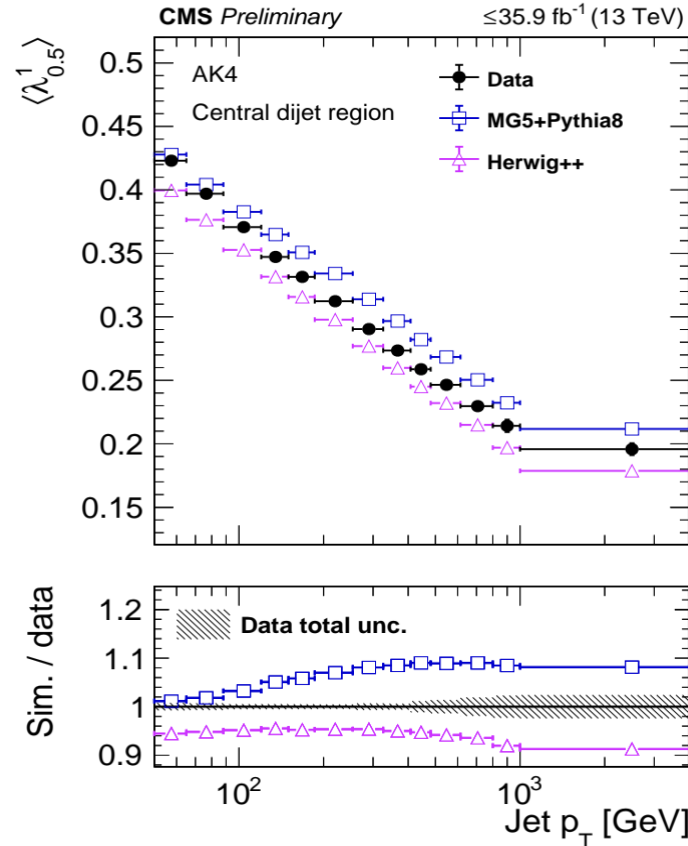
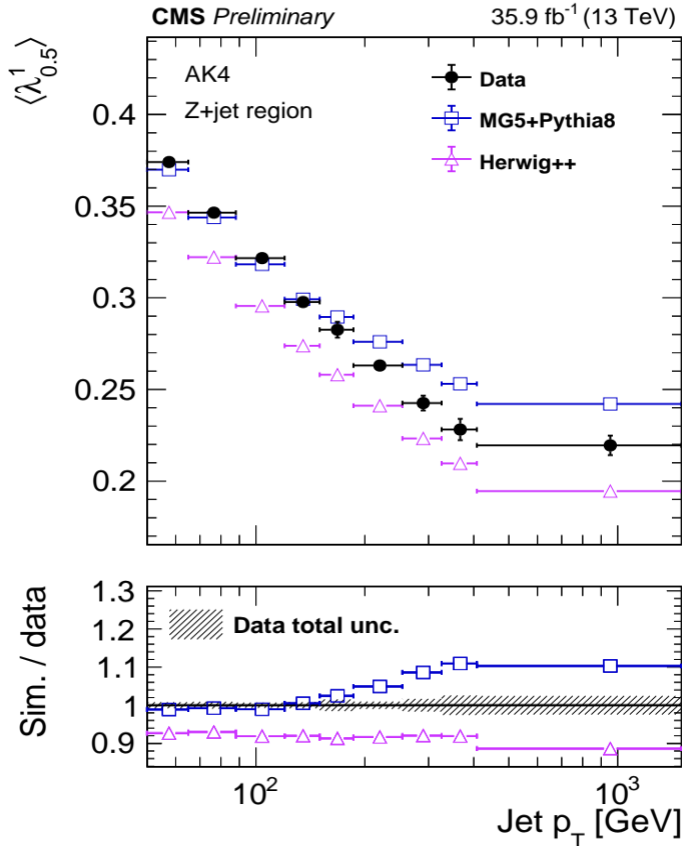
Radiation more spread out in gluon jet
→ Larger value of LHA

Differential distributions at particle-level

CMS-PAS-SMP-20-010

Quark-enriched sample

Gluon-enriched sample



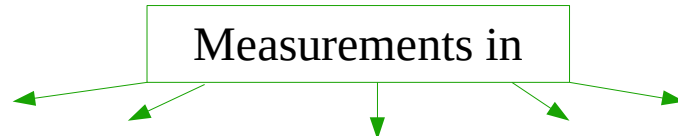
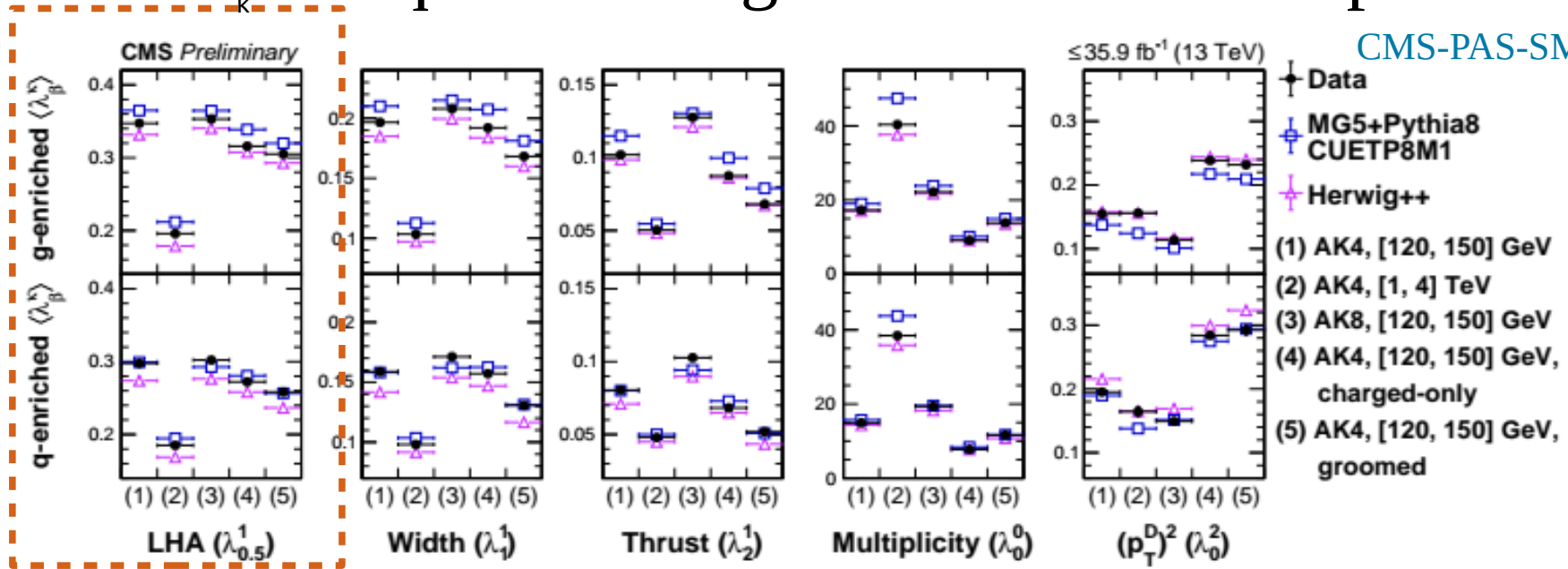
Good modeling of data by PYTHIA parton shower in quark-enriched samples

PYTHIA & HERWIG++ on opposite sides of data in gluon-enriched samples

HERWIG++ describes the p_{T} -dependence well but underestimates normalization

$\langle \lambda^\beta \rangle$ in quark- and gluon-enriched samples

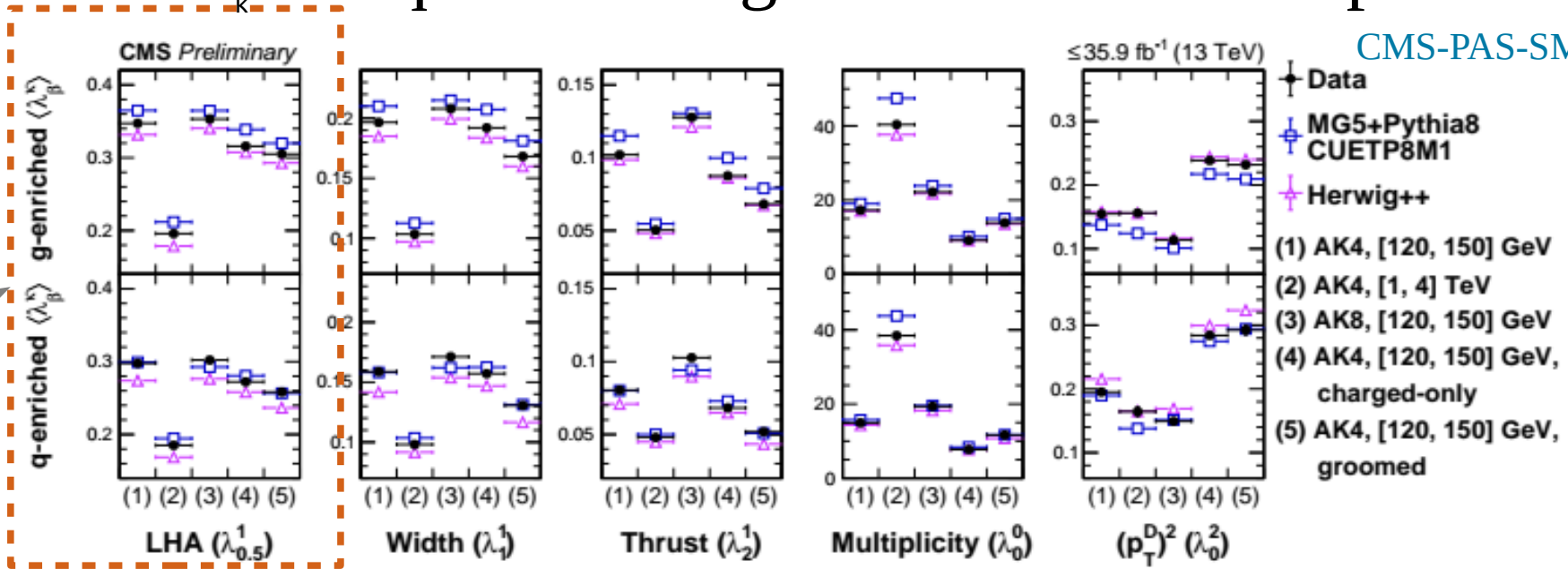
CMS-PAS-SMP-20-010



Event sample	Inputs from jet	Jet size	Grooming	Energy
Dijet (central)	All particles in jet	AK4	No grooming	In ranges of (ungroomed) jet p_T
Dijet (forward)	Charged particles only	AK8	Soft drop ($z_{\text{cut}} = 0.1, \beta = 0$)	(50 GeV \rightarrow 1 TeV)
Z+ jet				

$\langle \lambda^\beta \rangle$ in quark- and gluon-enriched samples

CMS-PAS-SMP-20-010



Event sample

Jet composition

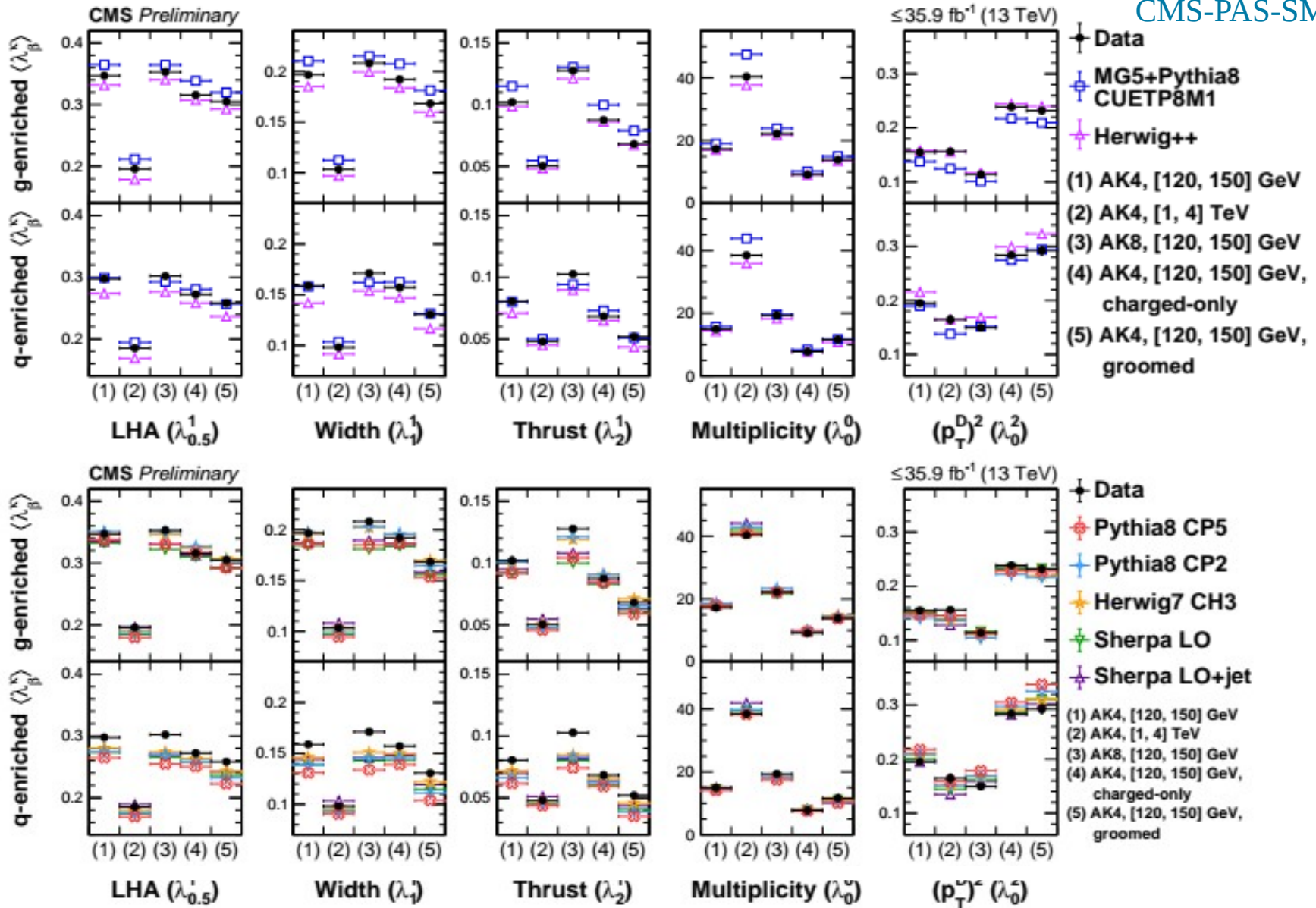
Dijet (central) \longrightarrow g-enriched

Dijet (forward) \longrightarrow q-enriched at [1, 4] TeV

Z+ jet \longrightarrow q-enriched at [120, 150] GeV

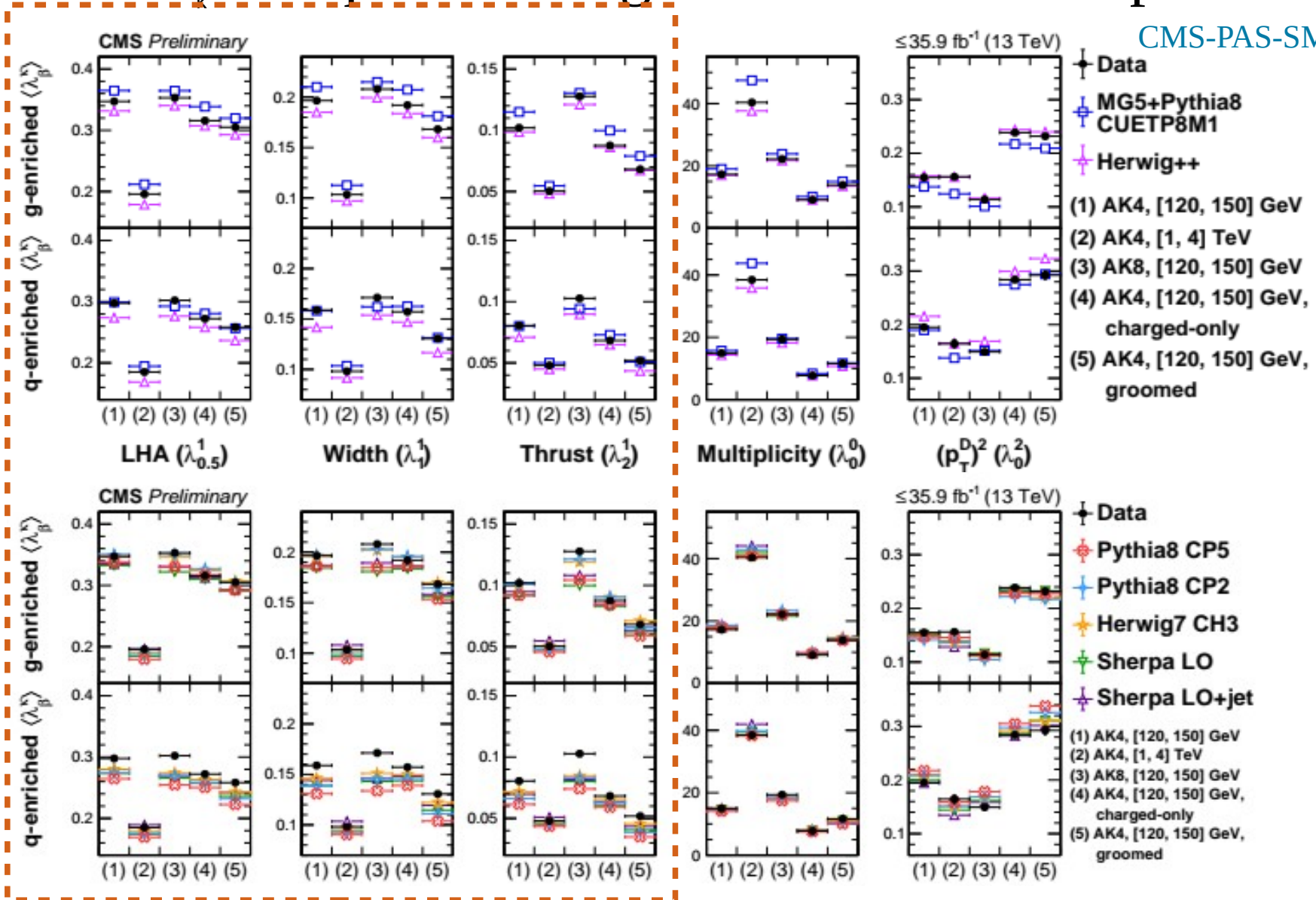
$\langle \lambda^\beta \rangle$ in quark- and gluon-enriched samples

CMS-PAS-SMP-20-010



$\langle \lambda^\beta \rangle$ in quark- and gluon-enriched samples

CMS-PAS-SMP-20-010

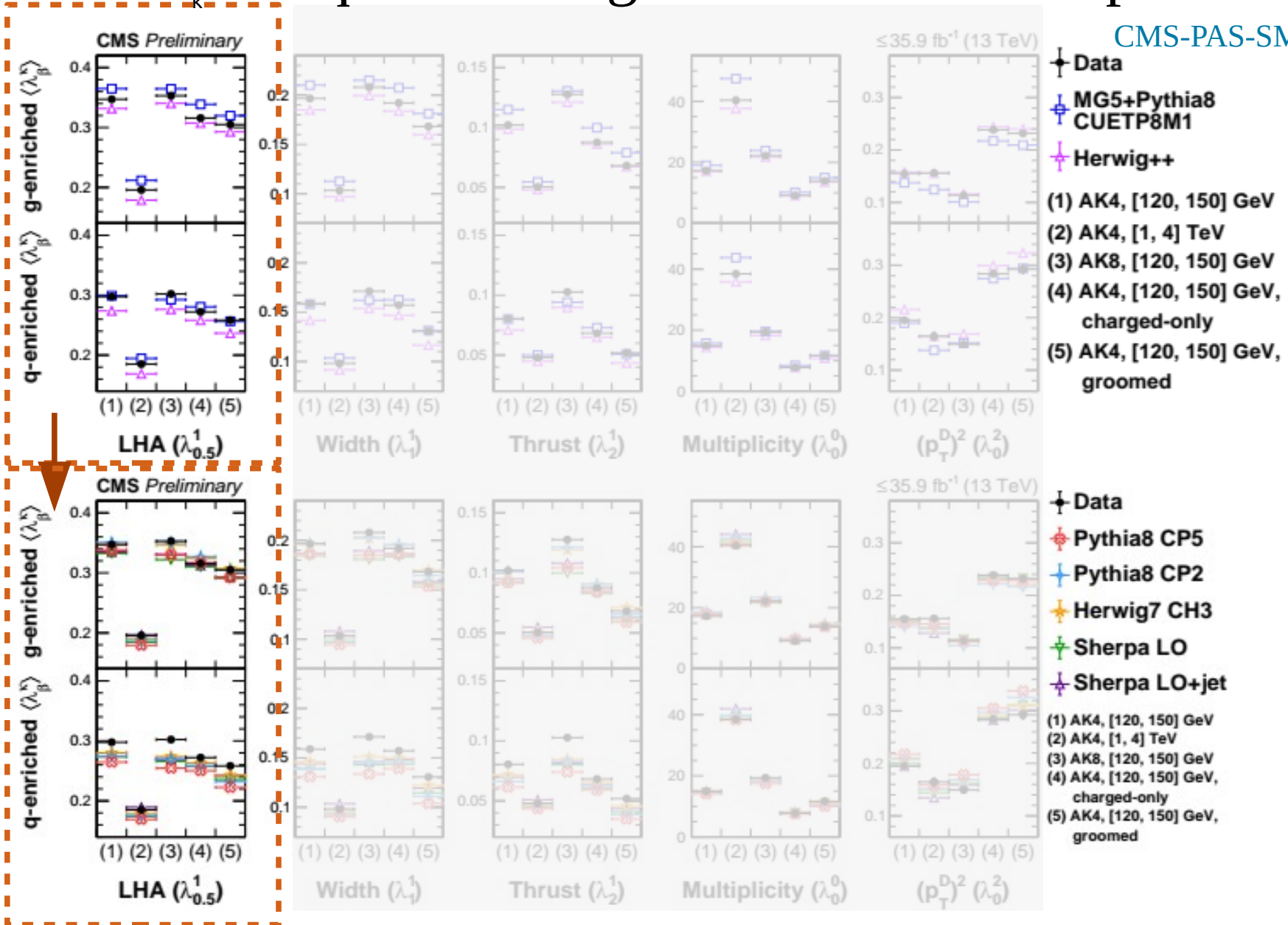


- IRC-safe variables not necessarily better modeled

=> Mismodeling by generators not only in non-perturbative region

$\langle \lambda^\beta \rangle$ in quark- and gluon-enriched samples

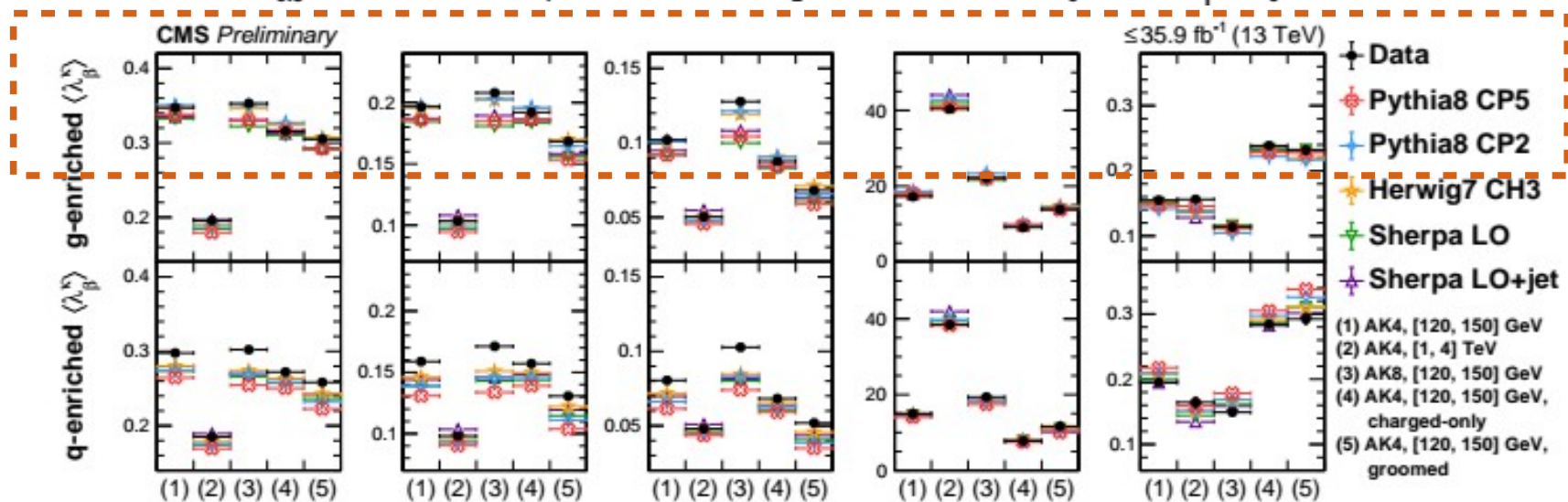
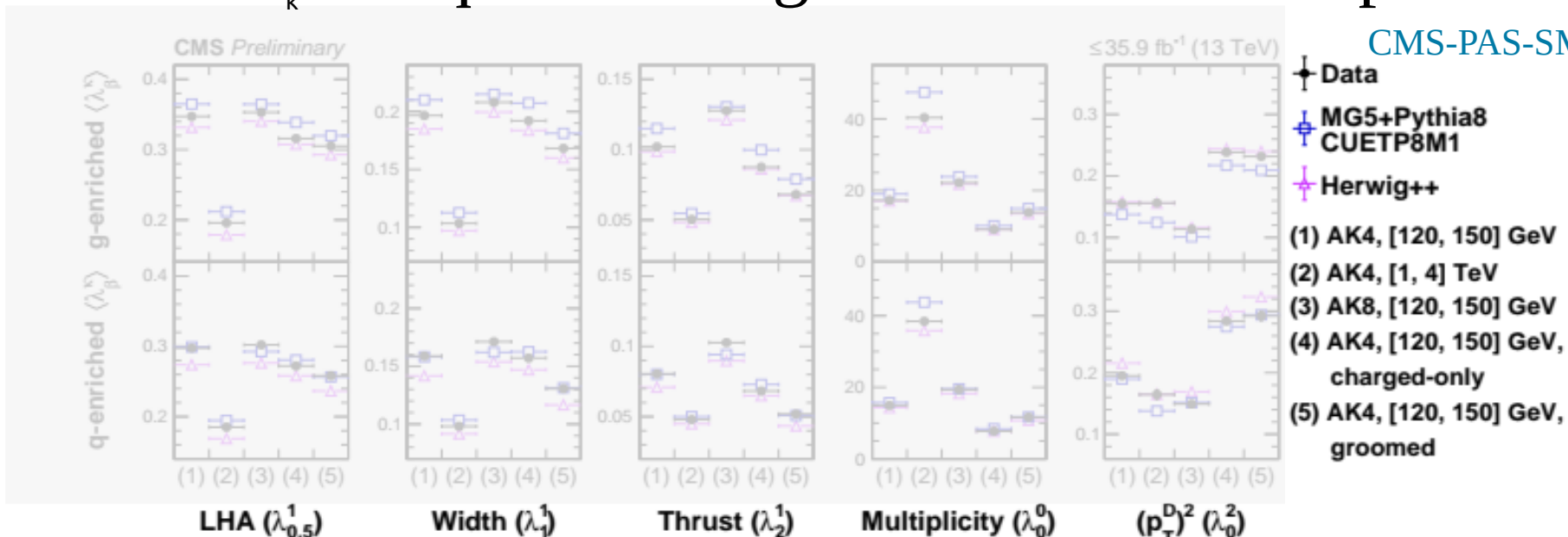
CMS-PAS-SMP-20-010



- Better modeling of gluon-enriched samples in modern generators + UE tunes

$\langle \lambda^\beta \rangle$ in quark- and gluon-enriched samples

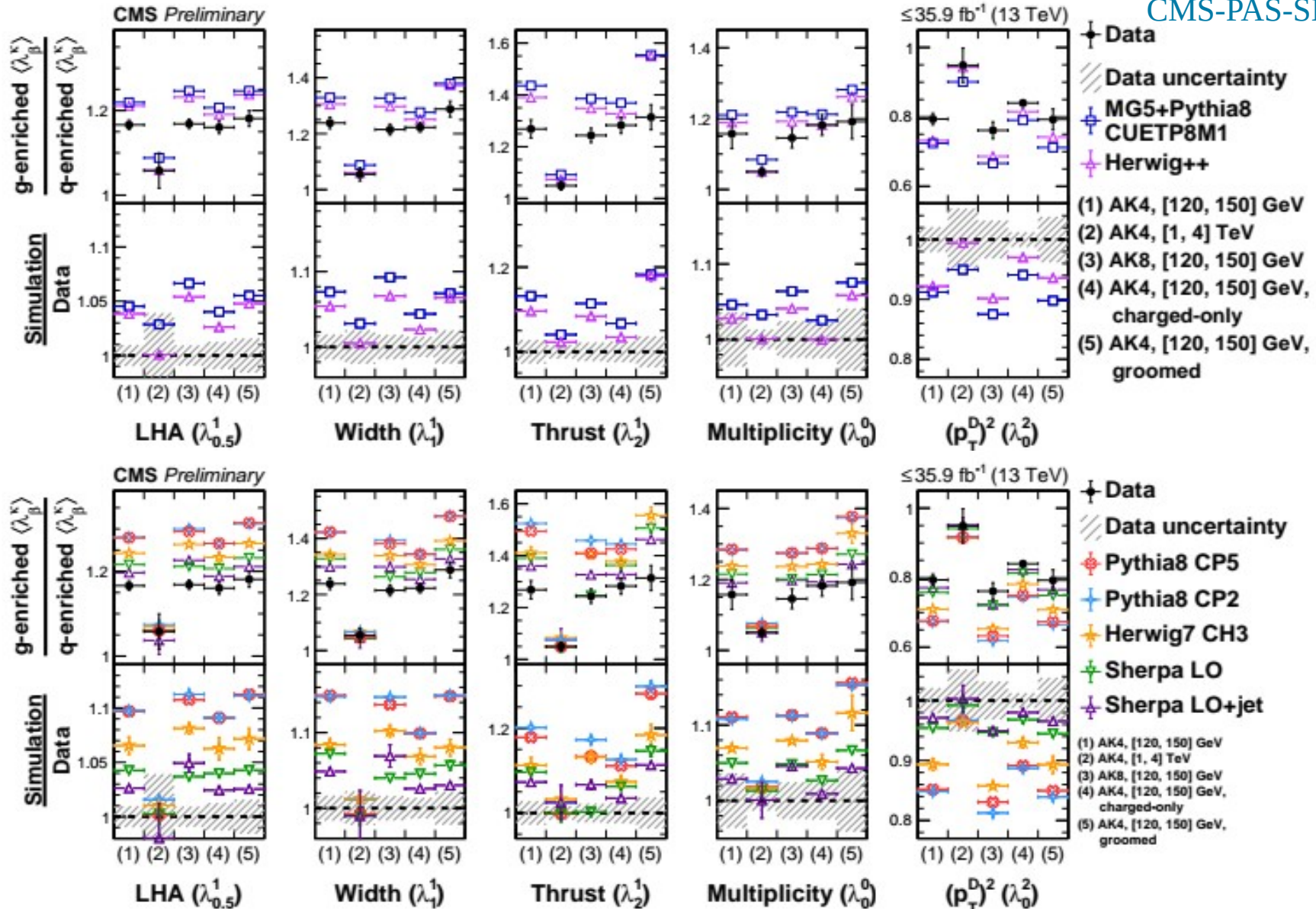
CMS-PAS-SMP-20-010



- CP2 tune describes gluon-enriched samples better than CP5 tune
(larger α_s & smaller color reconnection range in CP2)

Quark-gluon discrimination power in λ^{β}_K

CMS-PAS-SMP-20-010

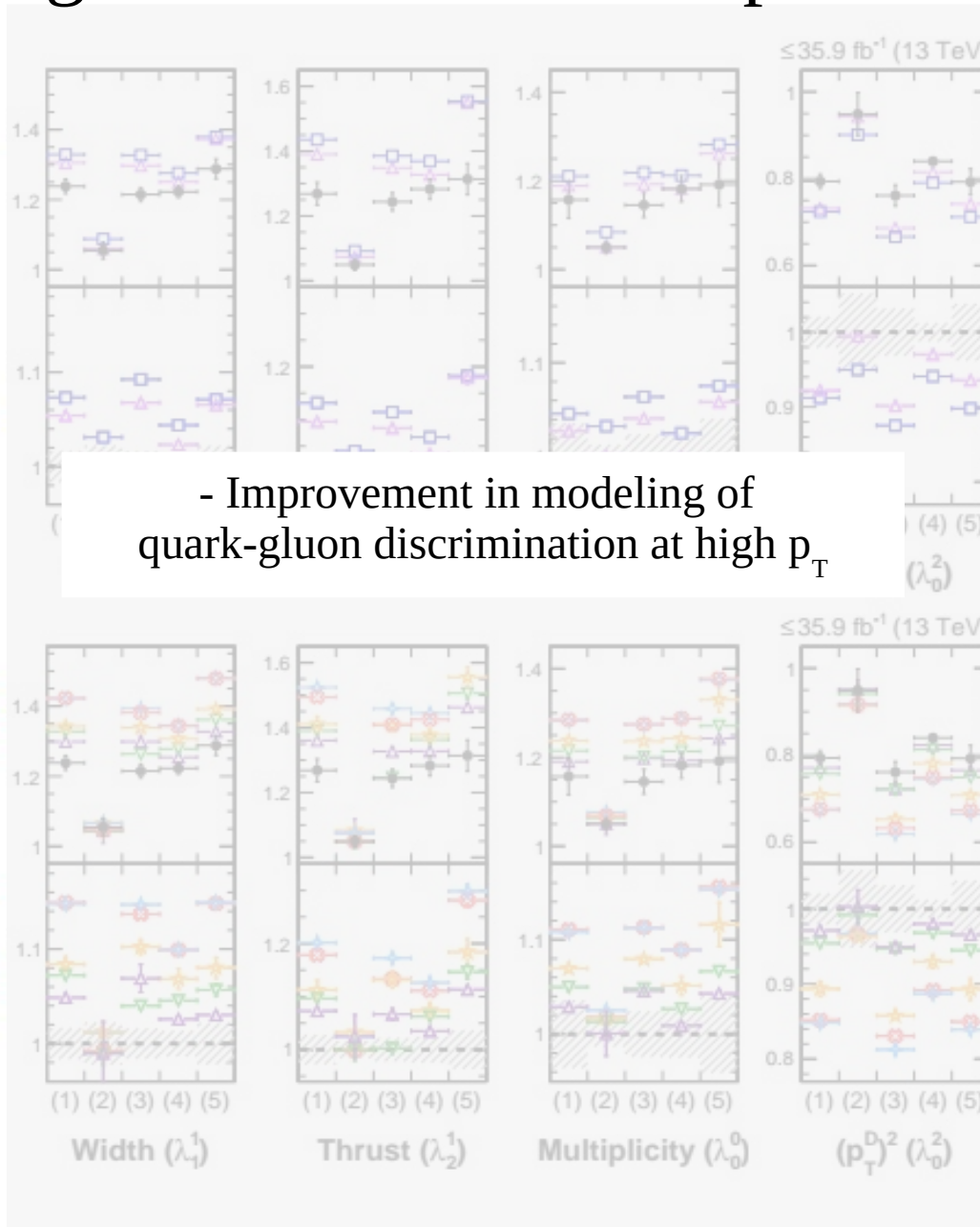
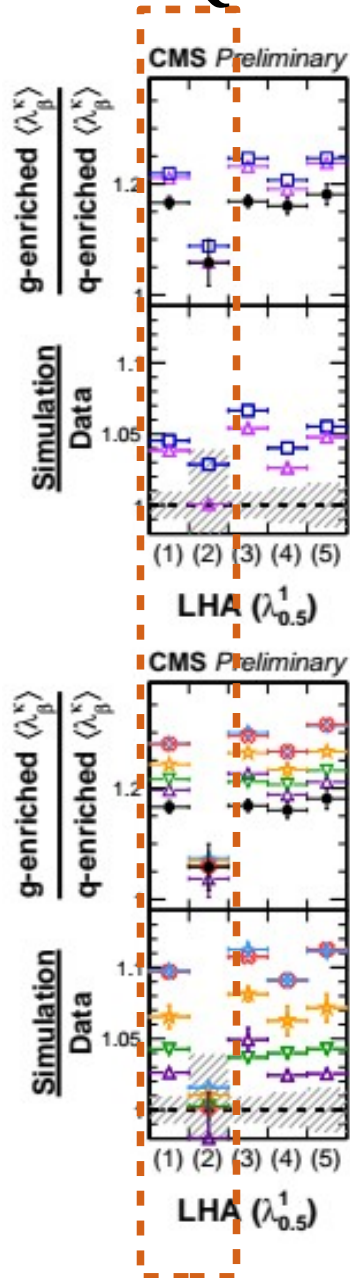


- Overestimation of quark-gluon discrimination by all the generators (except for λ^2_{γ})

- Sherpa LO+jet simulation is the closest to data

Quark-gluon discrimination power in λ^{β}_K

CMS-PAS-SMP-20-010



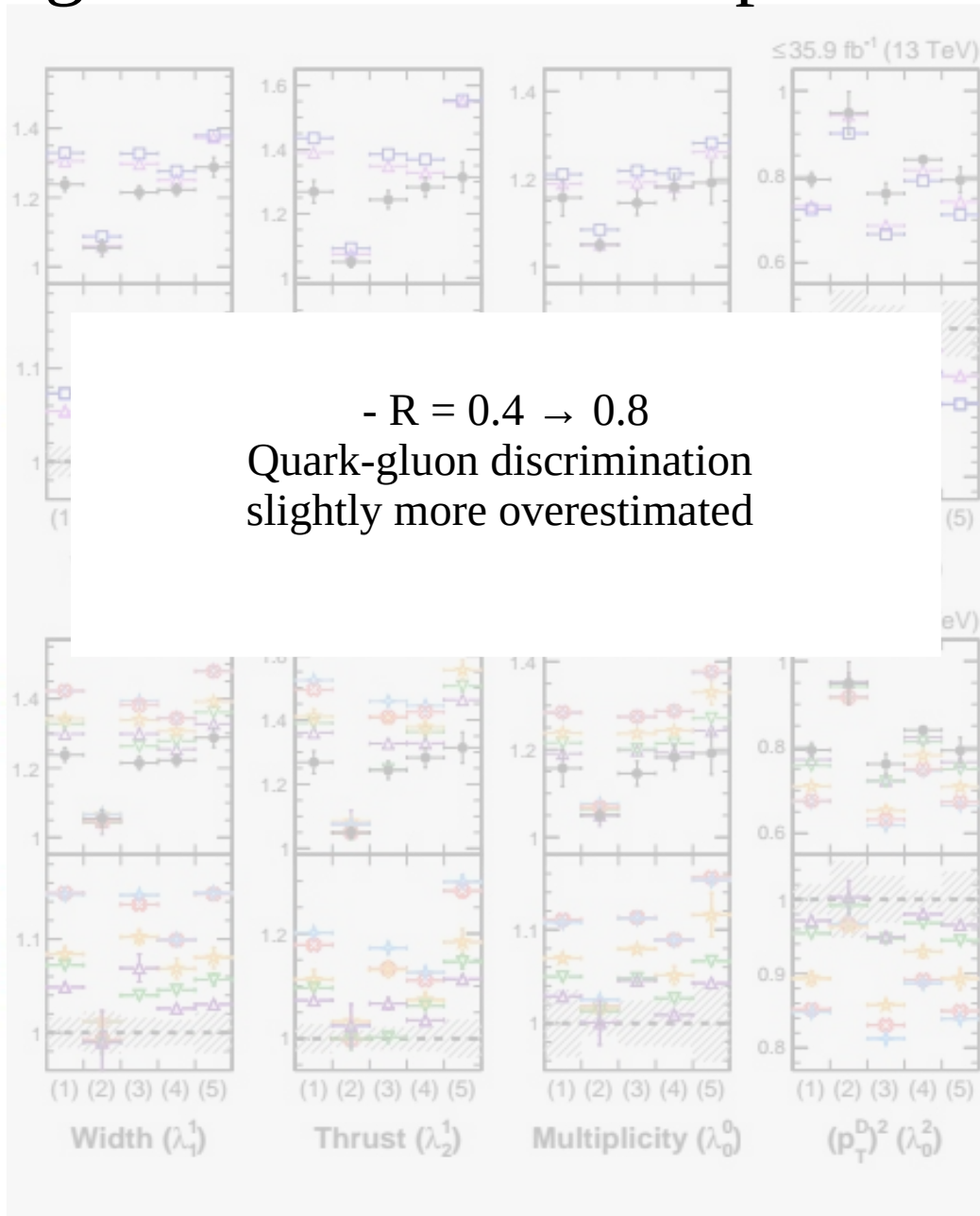
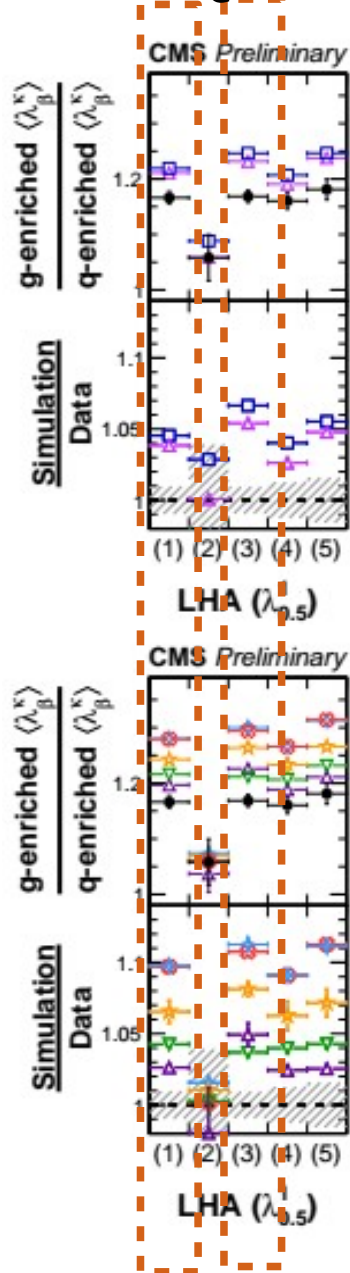
- Improvement in modeling of quark-gluon discrimination at high p_T

- ✦ Data
- ▨ Data uncertainty
- ✦ MG5+Pythia8 CUETP8M1
- ✦ Herwig++
- (1) AK4, [120, 150] GeV
- (2) AK4, [1, 4] TeV
- (3) AK8, [120, 150] GeV
- (4) AK4, [120, 150] GeV, charged-only
- (5) AK4, [120, 150] GeV, groomed

- ✦ Data
- ▨ Data uncertainty
- ✦ Pythia8 CP5
- ✦ Pythia8 CP2
- ✦ Herwig7 CH3
- ✦ Sherpa LO
- ✦ Sherpa LO+jet
- (1) AK4, [120, 150] GeV
- (2) AK4, [1, 4] TeV
- (3) AK8, [120, 150] GeV
- (4) AK4, [120, 150] GeV, charged-only
- (5) AK4, [120, 150] GeV, groomed

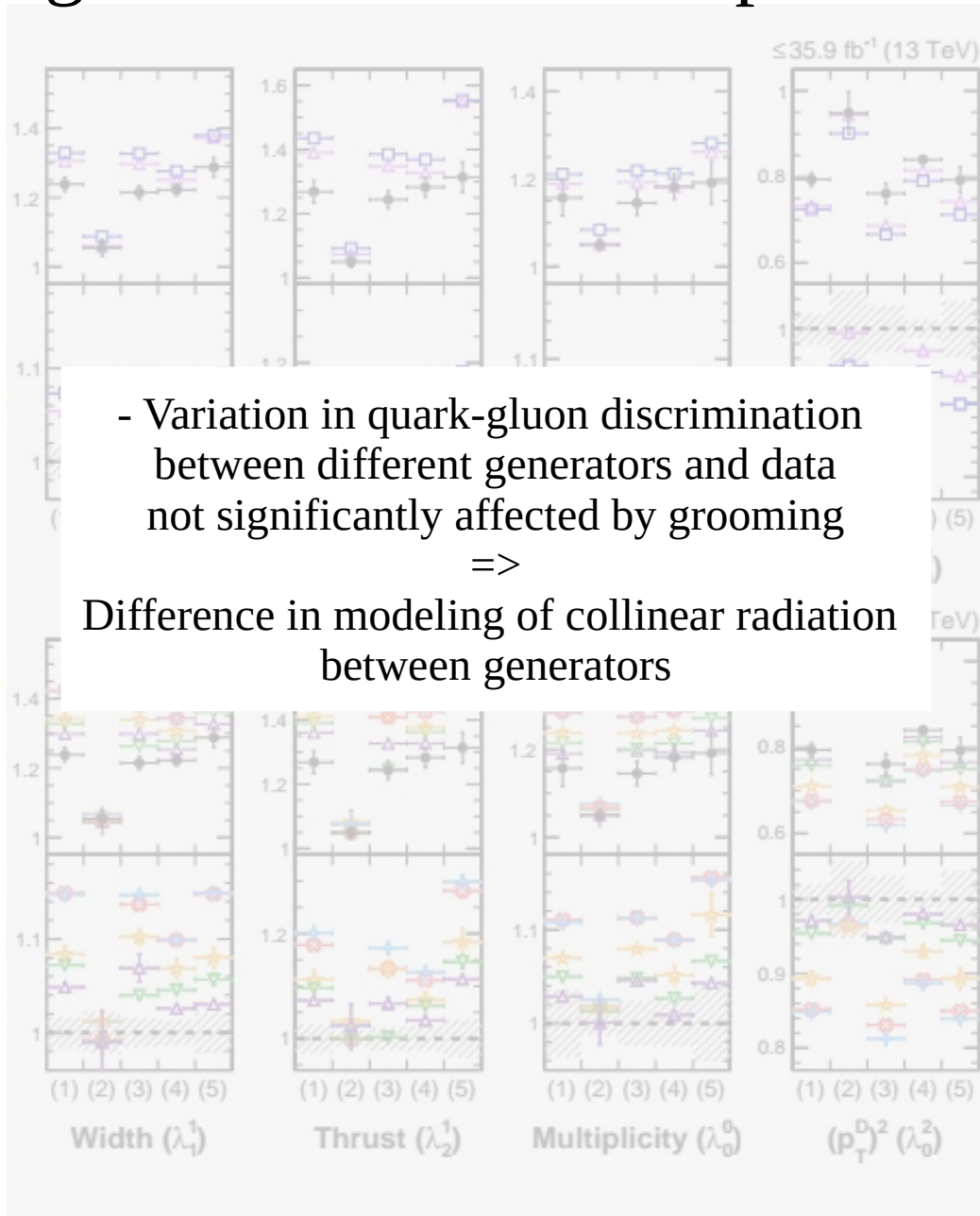
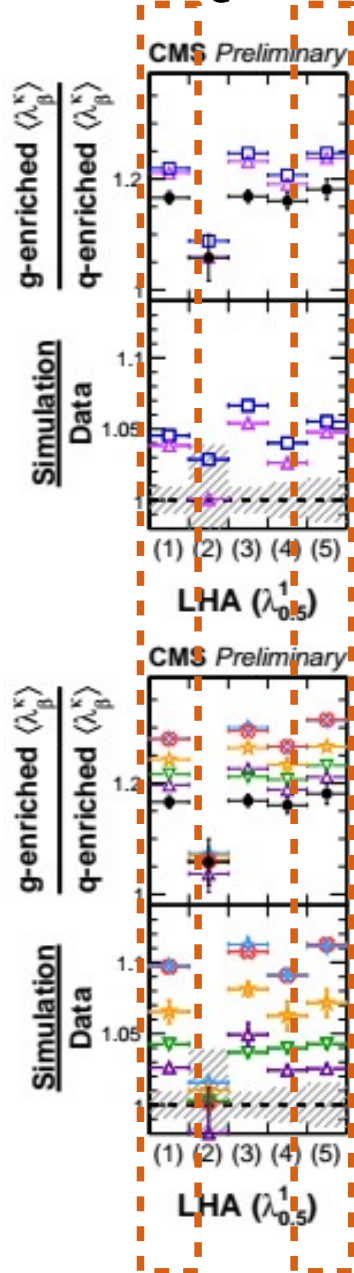
Quark-gluon discrimination power in λ^{β}_K

CMS-PAS-SMP-20-010



Quark-gluon discrimination power in λ^β

CMS-PAS-SMP-20-010



- Variation in quark-gluon discrimination between different generators and data not significantly affected by grooming

=>

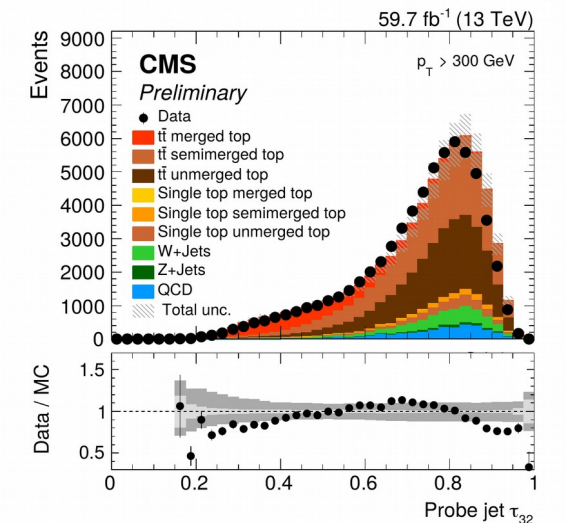
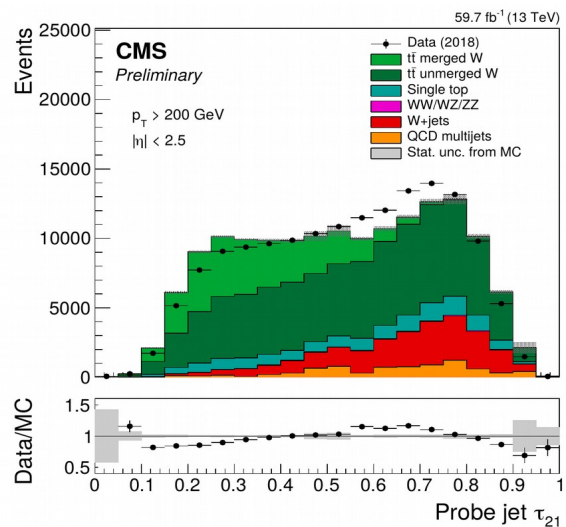
Difference in modeling of collinear radiation between generators

- ◆ Data
 - ▨ Data uncertainty
 - ◆ MG5+Pythia8 CUETP8M1
 - ◆ Herwig++
 - (1) AK4, [120, 150] GeV
 - (2) AK4, [1, 4] TeV
 - (3) AK8, [120, 150] GeV
 - (4) AK4, [120, 150] GeV, charged-only
 - (5) AK4, [120, 150] GeV, groomed
-
- ◆ Data
 - ▨ Data uncertainty
 - ◆ Pythia8 CP5
 - ◆ Pythia8 CP2
 - ◆ Herwig7 CH3
 - ◆ Sherpa LO
 - ◆ Sherpa LO+jet
 - (1) AK4, [120, 150] GeV
 - (2) AK4, [1, 4] TeV
 - (3) AK8, [120, 150] GeV
 - (4) AK4, [120, 150] GeV, charged-only
 - (5) AK4, [120, 150] GeV, groomed

W & top jet identification with n-subjettiness ratio

$\tau_{21} \rightarrow$ W tagging
 $\tau_{32} \rightarrow$ top tagging

$\tau_{n(n-1)} = \tau_n / \tau_{n-1}$ measures consistency of jet with n-prong structure

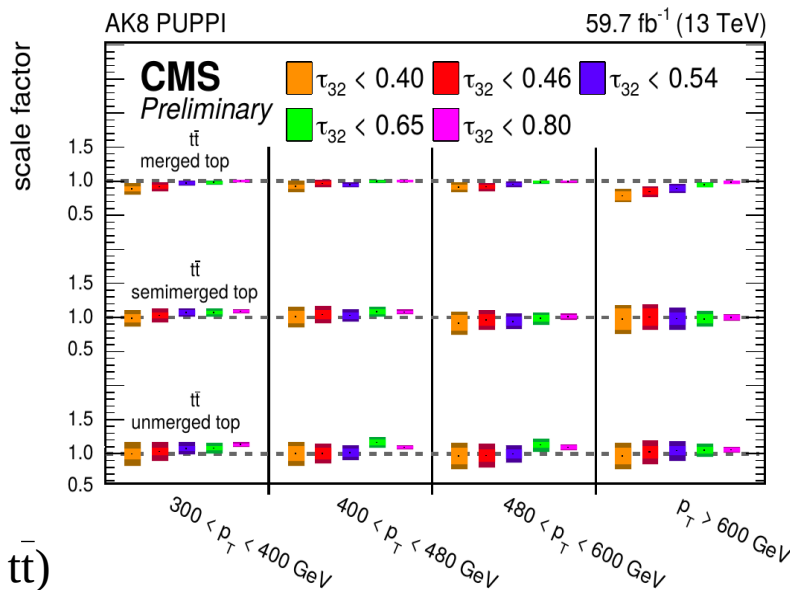
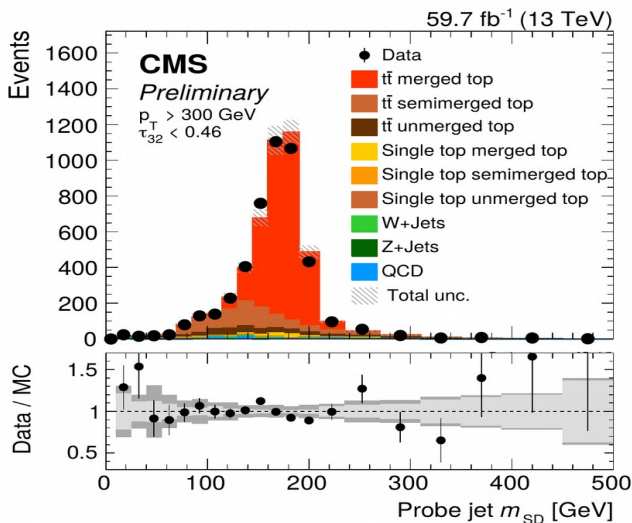
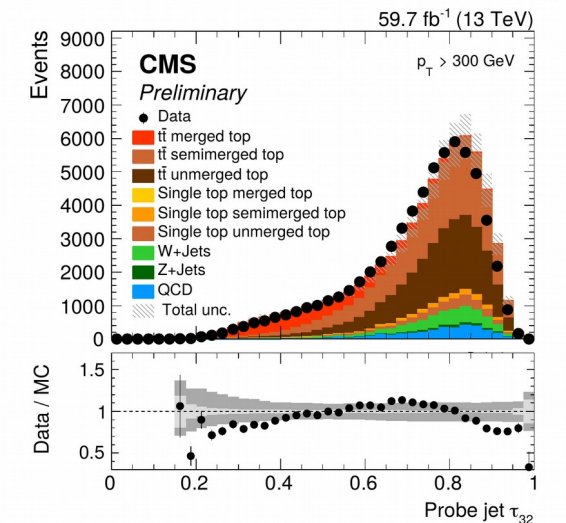
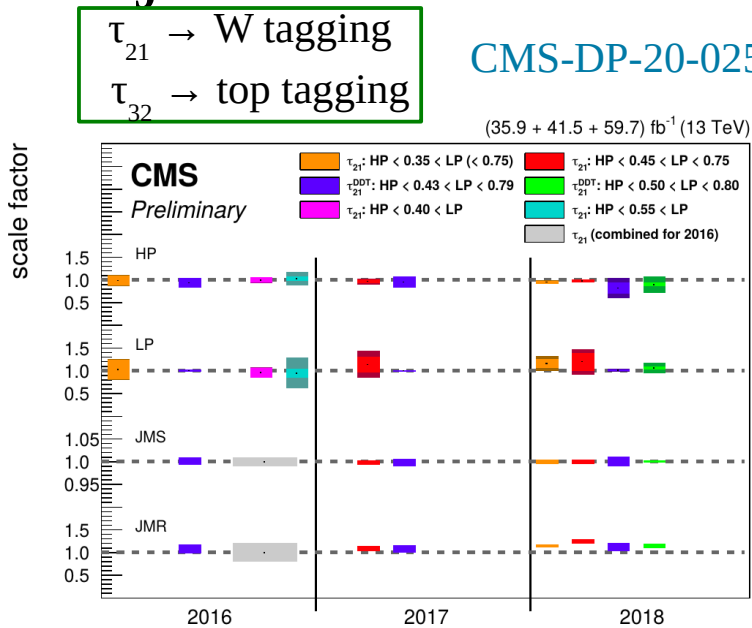
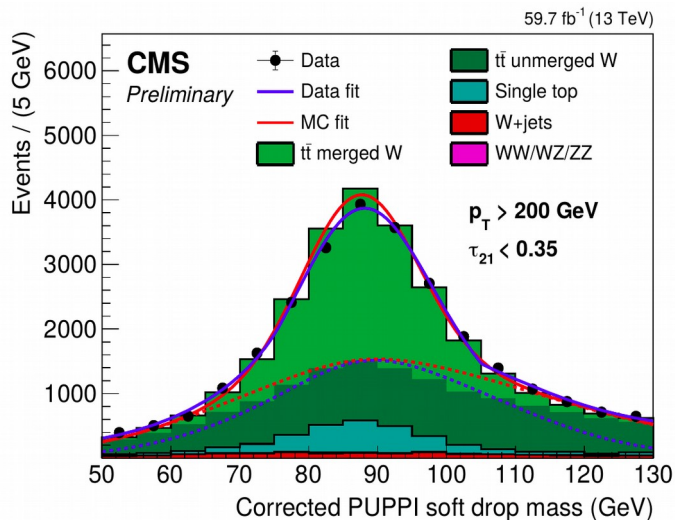
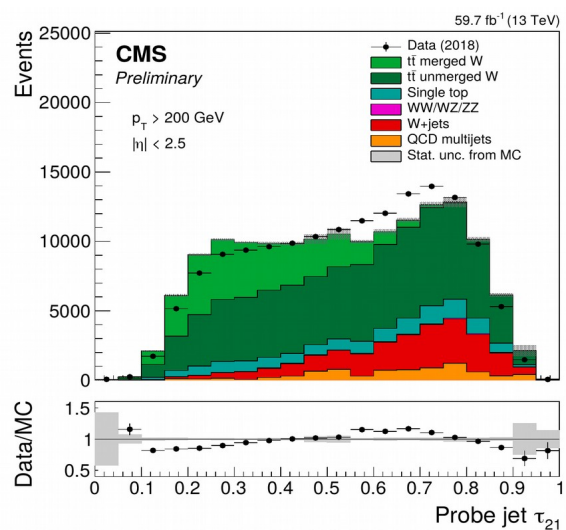


- Measurements in muon + jets events (dominated by semileptonic $t\bar{t}$)
- Room for improvement of description by simulation

W & top jet identification with n-subjettiness ratio

CMS-DP-20-025

$\tau_{n(n-1)} = \tau_n / \tau_{n-1}$ measures consistency of jet with n-prong structure



- Measurements in muon + jets events (dominated by semileptonic tt)

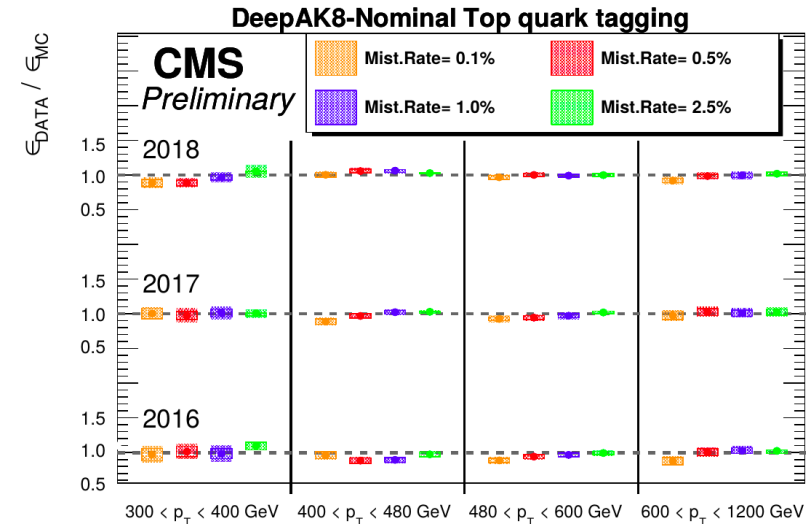
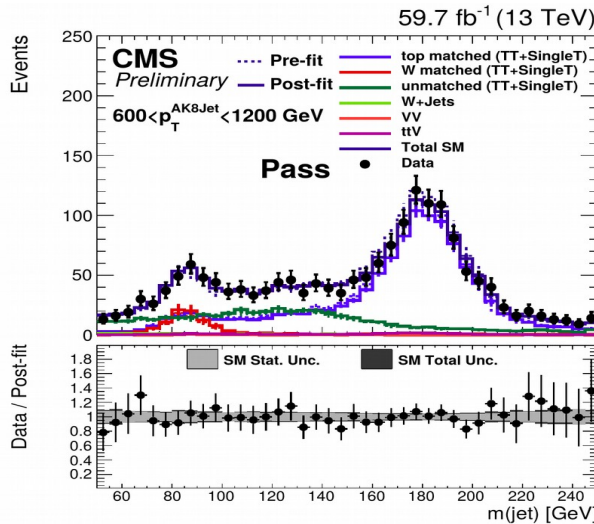
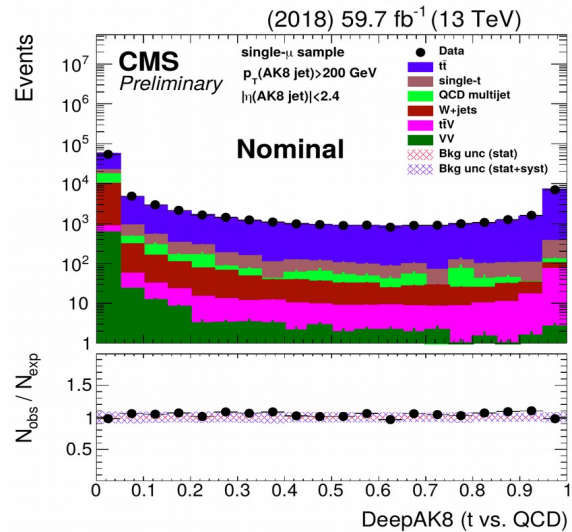
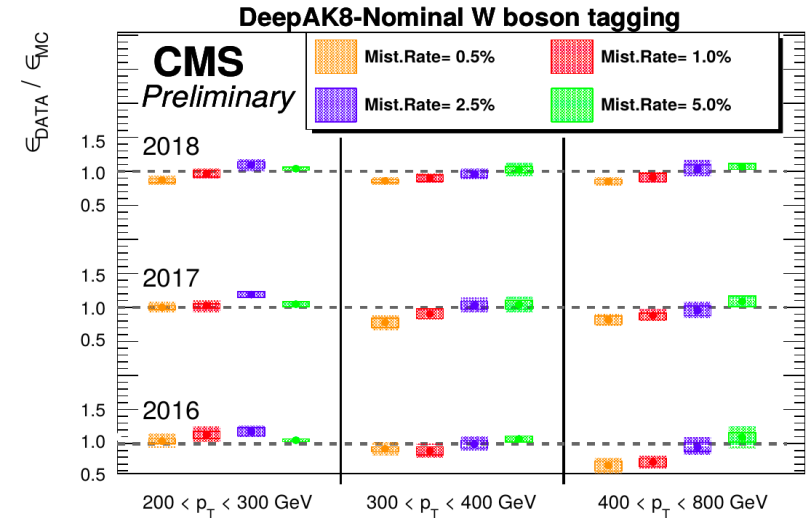
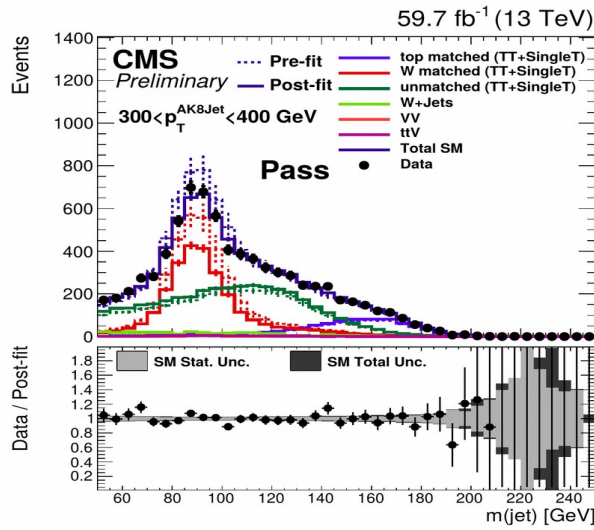
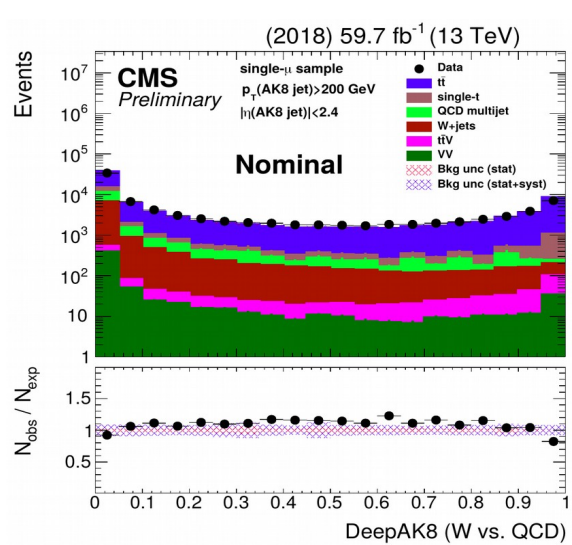
- Room for improvement of description by simulation

- Tagging efficiencies (measured using tag-and-probe method) are similar in data & simulation

W & top jet identification with DeepAK8 tagger

DNN-based tagger using (almost) all the particles & secondary vertices in AK8 jet

CMS-DP-20-025



- Measurements in muon + jets events (dominated by semileptonic tt)

- Moderately good description by simulation

See applications in [Anna Benecke's talk](#)

Details of DeepAK8 tagger in JINST 15 (2020) P06005

- Tagging efficiencies (measured using tag-and-probe method) are similar in data & simulation

Summary and Outlook

- A detailed study of jet substructure observables is performed

Useful for

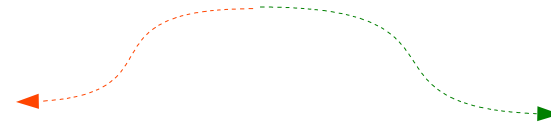
Better modeling of

Parton shower

Non-perturbative effects (hadronization, UE, ...)

pQCD calculations

Fixed order + resummation



Handle to reduce modeling uncertainty of particle identifiers
exploiting jet substructure

Improve measurements & searches

- Comparison with analytic calculation in progress

[JHEP 07 (2021) 076]

- Calibration measurement performed for heavy particle taggers

- More measurements are coming soon!

Summary and Outlook

- A detailed study of jet substructure observables is performed

Useful for

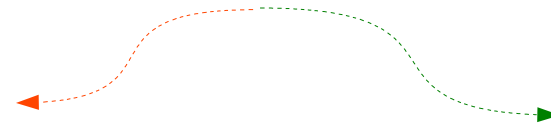
Better modeling of

Parton shower

Non-perturbative effects (hadronization, UE, ...)

pQCD calculations

Fixed order + resummation



Handle to reduce modeling uncertainty of particle identifiers exploiting jet substructure

Improve measurements & searches



- Comparison with analytic calculation in progress

[JHEP 07 (2021) 076]

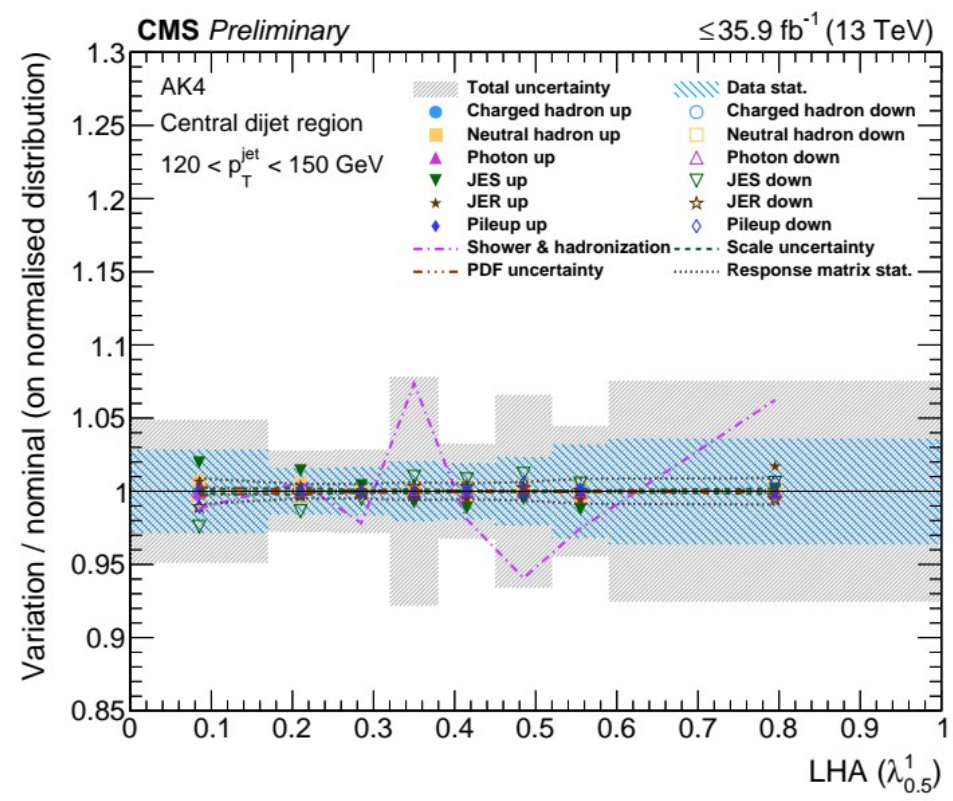
- Calibration measurement performed for heavy particle taggers

- More measurements are coming soon!



Extra material

Uncertainties in LHA



Showering+hadronization uncertainty is the dominant among all the systematic uncertainty sources



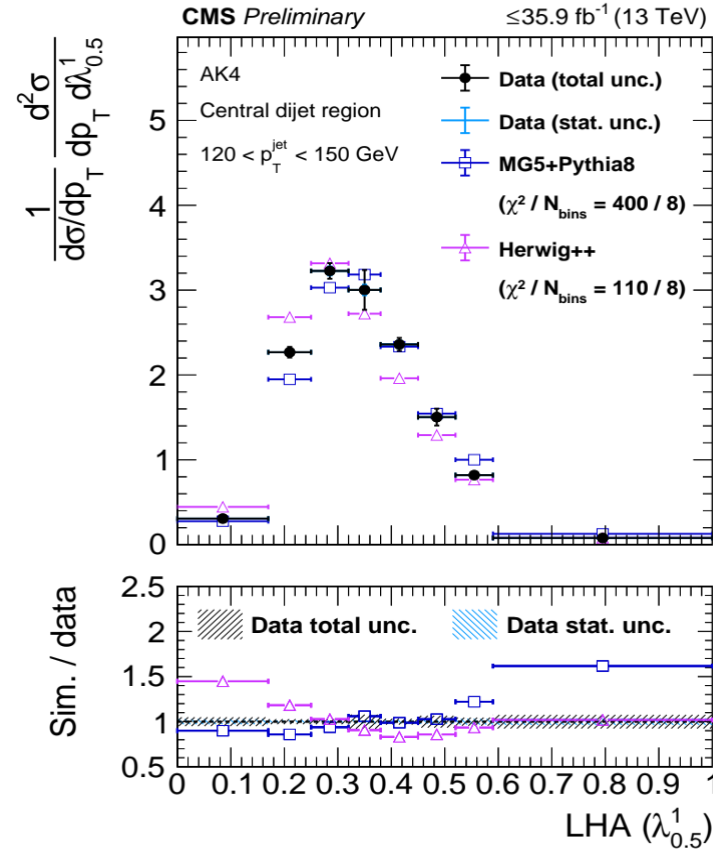
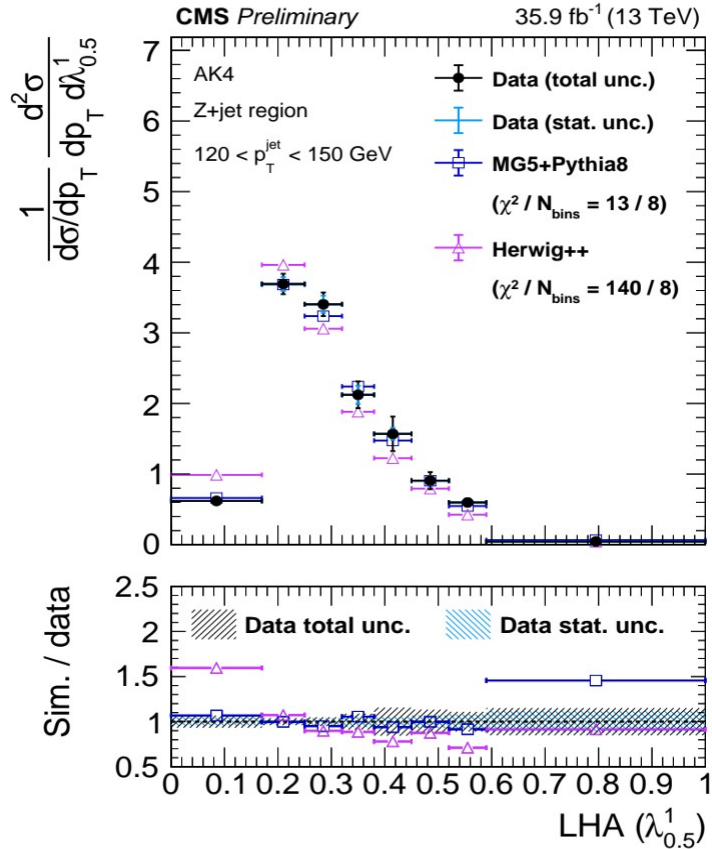
Differences of the unfolded distributions derived using response matrices constructed from MG5+Pythia8 and Herwig++

Differential distributions at particle-level

CMS-PAS-SMP-20-010

Quark-enriched sample

Gluon-enriched sample



Good modeling of data by PYTHIA parton shower in quark-enriched samples

PYTHIA & HERWIG++ on opposite sides of data in gluon-enriched samples

Top tagging efficiency

CMS-DP-20-025

Tagger	Working point	Signal efficiency [%]	Background efficiency [%]
AK8 PUPPI	$\tau_{32} < 0.40$	17	0.2
	$\tau_{32} < 0.46$	26	0.5
	$\tau_{32} < 0.54$	37	1.7
	$\tau_{32} < 0.65$	49	5.1
	$\tau_{32} < 0.80$	62	15.9
AK8 PUPPI + subjet btag	$\tau_{32} < 0.40$	16	0.1
	$\tau_{32} < 0.46$	23	0.3
	$\tau_{32} < 0.54$	33	0.6
	$\tau_{32} < 0.65$	43	1.8
	$\tau_{32} < 0.80$	53	5.3
HOTVR PUPPI	$\tau_{32} < 0.56$	37	2.6
DeepAK8	Mistag rate 0.1%	37	0.1
	Mistag rate 0.5%	52	0.5
	Mistag rate 1.0%	59	1.0
	Mistag rate 2.5%	67	2.5
DeepAK8 MD	Mistag rate 0.1%	28	0.1
	Mistag rate 0.5%	48	0.5
	Mistag rate 1.0%	57	1.0
	Mistag rate 2.5%	66	2.5

Table 1: The top tagging efficiencies including the respective mass windows are estimated from simulation in 2018 before the template fit for the AK8 PUPPI, HOTVR and DeepAK8 taggers. The efficiencies for signal are measured in $t\bar{t}$ events where the angular distance between the generated top and the probe jet is $\Delta R < 0.6$. Background efficiencies are measured using QCD multijet events. Only events are considered where the probe jet fulfills $480 < p_T < 600$ GeV. The exact values of efficiencies strongly depend on the selection applied. Therefore, the purpose of the presented numbers is to give a rough estimate and comparison between algorithms.

W tagging efficiency

CMS-DP-20-025

Tagger	Working point	Signal efficiency [%]	Background efficiency [%]
AK8 PUPPI	$\tau_{21} < 0.35$	53	2.0
	$\tau_{21} < 0.45$	69	4.7
	$\tau_{21}^{\text{DDT}} < 0.43$	12	0.1
	$\tau_{21}^{\text{DDT}} < 0.50$	32	0.6
DeepAK8	Mistag rate 0.5%	51	0.5
	Mistag rate 1.0%	62	1.0
	Mistag rate 2.5%	74	2.5
	Mistag rate 5.0%	79	5.0
DeepAK8 MD	Mistag rate 0.5%	38	0.5
	Mistag rate 1.0%	50	1.0
	Mistag rate 2.5%	66	2.5
	Mistag rate 5.0%	76	5.0

Table 2: The W tagging efficiencies including the respective mass windows are estimated from simulation in 2018 for the working points of the AK8 PUPPI and DeepAK8 taggers. The efficiencies for signal are measured in $Z' \rightarrow WW$ events where the angular distance between generated W and the probe jet is $\Delta R < 0.6$. Background efficiencies are measured using QCD multijet events. Only events are considered where the probe jet fulfills $300 < p_T < 500$ GeV. The exact values of efficiencies strongly depend on the selection applied. Therefore, the purpose of the presented numbers is to give a rough estimate and comparison between algorithms.